MODELLING STRAIN RATE SENSITIVE NANOMATERIALS' MECHANICAL PROPERTIES: THE EFFECTS OF VARYING DEFINITIONS.

A dissertation submitted in fulfilment of the requirements for the degree Magister Technologiae in Mechanical Engineering

In the Faculty of Engineering & Technology

Vaal University of Technology

Name of Student: Peter Baonhe Sob

Student Number: 213115549

M Tech: Mechanical Engineering

Supervisor: Prof. T. B. Tengen

Co-supervisor: Prof. A. A. Alugongo

Date: June 2016

Abstract:

Presently there exist a lot of controversies about the mechanical properties of nanomaterials. Several convincing reasons and justifications have been put forward for the controversies. Some of the reasons are varying processing routes, varying ways of defining equations, varying grain sizes, varying internal constituent structures, varying techniques of imposing strain on the specimen etc. *It is therefore necessary for scientists, engineers and technologists to come up with a clearer way of defining and dealing with nanomaterials' mechanical properties.* The parameters of the internal constituent structures of nanomaterials are random in nature with random spatial patterns. So they can best be studied using random processes, specifically as stochastic processes. In this dissertation the tools of stochastic processes have been used as they offer a better approach to understand and analyse random processes.

This research adopts the approach of ascertaining *the correct mathematical models to be used for experimentation and modelling*. After a thorough literature survey it was observed that size and temperature are two important parameters that must be considered in selecting the relevant mathematical definitions for nanomaterials' mechanical properties. Temperature has a vital role to play during grain refinement since all severe plastic deformation involves thermomechanical processes.

The second task performed in this research is to develop the mathematical formulations based on the experimental observation of 2-D grains and 3-D grains deformed by Accumulative Roll-Bonding and Equal Channel Angular Pressing. The experimental observations revealed that grains deformed by Accumulative Roll-Bonding and Equal Channel Angular Pressing are elongated when observed from the rolling direction, and transverse direction, and equiaxed when observed from the normal direction. In this dissertation, the different experimental observations for the grain size variants during grain refinement were established for 2-D and 3-D grains. This led to the development of a stochastic model of grain-elongation for 2-D and 3-D grains.

The third task was experimentations and validation of proposed models. Accumulative Roll-Bonding, Equal Channel Angular Pressing and mechanical testing (tensile test) experiments were performed. The effect of size on elongation and material properties were studied to validate the developed models since size has a major effect on material's properties.

The fourth task was obtaining results and discussion of theoretical developed models and experimental results. The following facts were experimentally observed and also revealed by the models. Different approaches of measuring grain size reveal different strains that cannot be directly obtained from plots of the corresponding grain sizes. Grain elongation evolved as small values for larger grains, but became larger for smaller grains. Material properties increased with elongation reaching a maximum and started decreasing as is evident in the Hall-Petch to the Reverse Hall-Petch Relationship. *This was alluded to the fact that extreme plastic straining led to distorted structures where grain boundaries and curvatures were in "non-equilibrium" states*.

Overall, this dissertation contributed new knowledge to the body of knowledge of nanomaterials' mechanical properties in a number of ways. The major contributions to the body of knowledge by his study can be summarized as follows:

(1) The study has contributed in developing a model of elongation for 2-D grain and 3-D grains. It has been generally reported by researchers that materials deformed by Accumulative Roll-Bonding and Equal Channel Angular Pressing are generally elongated but none of these researchers have developed a model of elongation. Elongation revealed more information about "size" during grain refinement.

(2) The Transmission Electron Microscopy revealed the grain shape in three directions. The rolling direction or sliding direction, the normal direction and the transverse direction. Most developed models ignored the different approaches of measuring nanomaterials' mechanical properties. Most existing models dealt only with the equivalent radius measurement during grain refinement. In this dissertation, the different approaches of measuring nanomaterials' mechanical properties have been considered in the developed models. From this dissertation an accurate correlation can be made from microscopy results and theoretical results.

(3) *This research has shown that most of the published results on nanomaterials' mechanical properties may be correct although controversies exist when comparing the different results*. This research has also shown that researchers might have considered different approaches to measure nanomaterials' mechanical properties. The reason for different results is due to different approaches of measuring nanomaterials' mechanical properties as revealed in this research. Since different approaches of measuring nanomaterials' mechanical properties led to different obtained results, this justify that most published results of nanomaterials' mechanical properties may be correct. This dissertation revealed more properties of nanomaterials that are ignored by the models that considered only the equivalent length.

(4) This research has contributed to the understanding of nanomaterials controversies when comparing results from different researchers.

Keywords: Nanostructured materials, grain size variants, elongation, mechanical properties, yield stress, temperature, strain rate sensitivity, activation volume.

Declaration of Dissertation

I declare that this dissertation is my own unaided work. It is being submitted for the degree M Tech in Mechanical Engineering at the Vaal University of Technology, Vanderbijlpark, South Africa. It has not been submitted before for any degree or examination at any other University.

Signature of Candidate……

Date: June 2016

Statement 1

This dissertation is being submitted in fulfilment of the requirements for the degree of Magister Technologiae: Mechanical Engineering

Signature of Candidate……

Date: June 2016

Statement 2

This dissertation is the result of my own independent work/investigation, except where otherwise stated. Other sources are acknowledged by giving explicit references. A list of references is appended.

Signature of Candidate……

Date: June 2016

Statement 3

I hereby give consent for my dissertation, if accepted, to be available for online publication, photocopying and for interlibrary loan, and for the title and summary to be made available to outside organisations.

Signature of Candidate……

Date: June 2016

Publications and Proceedings Arising From this Dissertation

1. Stochastic effect of grain elongation on nanocrystalline materials yield stress produced by Accumulative roll-bonding (ARB). *Published online by South Africa Conference of Computational and Applied Mechanics (SACAM 2014) paper number SACAM 046. Date of publication 14-16 January 2014 at Lord Charles Hotel Stellenbosch South Africa.*

2. The effect of deformation activation volume, strain rate sensitivity and processing temperature of grain size variants. *International Journal of Mechanical, Aerospace, Industrial, Mechatronics and Manufacturing Engineering Vol:9, No:11, 2015.*

3. Determination of strain rate sensitivity (SRS) for grain size variants on nanocrystalline materials produced by ARB and equal channel angular pressing (ECAP). *International Journal of Chemical, Molecular, Nuclear, Materials and Metallurgical Engineering Vol:9, No:12, 2015*

4. The effect of different approaches of measuring grain size on nanomaterials' mechanical properties. Paper currently under review for journal publication.

Upcoming Publications

5. Cracks Propagation as a Function of Grain Size Variants on Nanocrystalline Materials Yield Stress Produced by Accumulative Roll-Bonding

Abstract

Cracks are usually observed at the edge of a material being deformed by Accumulative roll bonding from conventional materials to nanostructure materials. The observed cracks usually propagate in the materials during grain refinement. This crack propagation affects the yield stress of nanocrystalline materials. In this study, the impacts of crack propagation as a function of grain size variants on nanocrystalline materials' yield stress is investigated for a material deformed by Accumulative roll-bonding. The study focuses on experimental data and theoretical concepts of severe plastic deformation and cracks processes in nanocrystalline materials. The study also focuses on high yield stress that leads to material failure during severe plastic deformation. The study also suggests a theoretical model that shows the generation of nanomaterials cracks during grain refinement as a function of grain size variants. In the model the cracks propagate on nanocrystalline materials due to the applied stress. The model predicts that the generation of cracks as a function of grain size variants impacts the energy level in nanocrystalline materials.

Keywords: nanostructured, grain size variants, stress, crack, energy

6. **The Effects of Grain Size Variants on Fracture Toughness of Nanocrystalline Materials Produced by Accumulative roll-bonding**

Abstract

Although several researchers have investigated fracture behaviour of nanocrystalline (nc) materials, difficulties in measuring fracture toughness have discouraged researchers in gaining insight on the relationships between microstructure and fracture resistance. This study focuses on cracks that occur during Accumulative roll-bonding (ARB). The fracture toughness is studied as a function of the grain size variants during deformation of conventional materials to nanostructure materials. The results revealed that the fracture toughness increases during grain refinement. The results show that the fracture toughness increases at different rates in nc materials when measured as a function of different grain size variants when the grain sizes dramatically decrease. The increase in fracture toughness during grain refinement of nc materials was due to diffusion of materials from the crack region. As materials are being diffused from the crack region, grain boundary (GB) dislocations took place and more material moved away from the crack section as the crack in the material increases during grain refinement.

Keywords: Fracture toughness, grain size variants, nanostructured materials,

7. **The Effects of the Size Variants of Nanocrystalline Materials Produced by Accumulative Roll-Bonding on their Energy, Thermodynamics and Mechanical Properties**

Abstract

This research extends the first law of thermodynamics which provides us with the relationship between heat, work and energy content of a system. A general principle is proposed to evaluate the internal energy of nanocrystalline materials deformed by Accumulative roll bonding (ARB). The interrelation between the thermodynamic, energy and properties of nanomaterials is presented and the relationship between the variation of properties and grain size variants of nanomaterials is explained based on 3-D grains deformed by ARB. The results of the study agree with molecular dynamics (MD) simulation, thermodynamics and experimental results. The results, however, indicate that the grain refinement follows an inverse proportional relationship between grain size variants and internal energy and temperature which is in good agreement with experimental results. This research is of significance in investigating the effects of size variants of nanomaterials on mechanical properties and gives a new approach for studying their energy, thermodynamics and mechanical properties.

Keywords: nanostructured, grain size variants, thermodynamics, grain boundary, internal energy,

8. Stochastic Model of Nanocrystalline Materials Energy Produced by Accumulative Roll-Bonding

Abstract

Energy is the quantity that measures a combination of efforts. For macroscopic systems energy is often defined as the "ability to perform work" by a system under consideration. The concept of energy is well understood for macro systems and not understood for nano-systems since the term "work" required a more precise definition than it is generally understood in macroscopic systems. This research develops a stochastic model of energy of nanocrystalline (nc) materials produced by Accumulative roll-bonding (ARB) by considering the intrinsic influence of bond energy on the microstructure and the change of internal energy due to "work" and heat supplied during the deformation of nanostructure material. The developed model considered the variation of energy for grain size variants for a 3-D grain deformed by ARB. The developed models also considered the work done in the deformation of nanostructure materials and also the intrinsic influence of bonding energy and the lattice distortion energy during grain refinement of 3-D grains. The stochastic nature of grain size was also considered and lognormal distribution was used.

The performed "work" in nc materials impacts the energy in the material. The result indicates that grain refinement follow an inverse proportional relationship with grain size variants during grain refinement. The results also revealed that the energy increases with decrease in grain size for the grain size variants. The results however revealed the variation of nanomaterial energy for grain size variants during grain refinement.

Keywords: energy, nanostructure, work, size variants

Acknowledgement

The academic journey, almost always, is painful and often much too difficult to bear alone. As such, there are several people that made my experience bearable, and it is only proper to acknowledge them because without their support and encouragement, you would not be reading this dissertation today (there would have not been a dissertation after all).

Praise to **God for His unconditional love and blessings** throughout my research.

Firstly I would like to thank my family. It is with their love and support throughout the years that this work is possible. They have always been there for me and I am grateful for their love and generosity.

Next I would like to thank my supervisors **Prof T. B. Tengen** whose technical expertise converted my wild imagination into a fine art. Special thanks to my co-supervisor **Prof A. A. Alugongo for his contributions**. Their help, wisdom and guidance over the years are unappreciable and without it I would not have been where I am today.

To the **Vaal University of Technology, Vanderbijlpark, South Africa and the Faculty of Engineering and Technology,** what can I say, as graduate students we are truly fortunate. I thank you for the knowledge you have passed on which will brighten to all eternity. I would like to thank the management of **Trade Fin Engineering, Vanderbijlpark** for their support during my experimentations.

Special Thanks to my Brother **Rev. Fr. Alexander Sob Nougi** Catholic Education Secretarial for the Diocese of Buea Cameroon (CES). I would like to thank **Rev. Dr Fr. George Nkeze** Pro-chancellor University Institute of the Diocese of Cameroon Buea (UIDB), **Rev. Fr. Basil Sede** President of (UIDB) and **Rev. Fr Dr Edward Ngalamen** Parish Priest of Likomba Parish Cameroon.

I would like to express my thanks to **Vaal University of Technology and the National Research Foundation (NRF)** for their financial support.

To my fellow graduate students, thank you for the great company throughout the years. I wish you all the best of luck and God's blessings.

In addition I would like to thank my brothers, sisters and my friends for their moral and spiritual support.

I would like to thank my wife **Ngobena Nadege Sob** and My daughters **Baonhe Sob Nadia and Ngo-Nougi Rosie Purity Sob** for their love and understanding throughout my research in South Africa

Finally I am ever grateful for the life of my dad **Mr. Sob Paul Zeno** (R.I.P) and my mum **Mrs. Sob** may God bless them all.

Dedication

To

My dad (Sob Paul Zeno RIP)

My mum (Ngo- Noug Anne Marie Sob)

My wife and daughters

Mrs Ngobena Nadege Sob, Baonhe Nadia Sob and Ngo-Nougi Rosie Purity Sob

My brothers
Rev Fr Alexander Nougi Sob Catholic Education Secretarial Diocese of Buea Cameroon

Mr Noug Rene Sob
Mr Mandjund Paul Sob

Mr Noug Christian Sob

My sisters

Mrs Meh Florence Sob

Ngo-Ngi Bernadette Sob (RIP)

Miss Ngo-Noug Anne Marie Sob

My supervisor
Prof Thomas B. Tengen
Industrial Engineering Vaal University of Technology
My co-supervisor
Prof A. A. Alugongo
Head of Mechanical Engineering Vaal University of Technology

Table of Contents

Chapter Two: Literature Review

Chapter Three: Research Design and Methodology

List of Figures

List of Tables

LIST OF SYMBOLS AND ACRONYMS

Curvature driven Grain Boundary Migration mechanism	GBM
Grain Boundary	GB
Grain Boundaries	GBs
Grain boundary mobility	M(r,T)
Increment of Weiner (continuous) Process	dW(t)
Increment of stochastic counting process	dN(t)
Increment of number of Coalescence events or mechanisms of grains within infinite small time interval	dN(r,t)
Material mean yield stress	σ
Material yield stress	σ(E(r),CV(r)
Strain	ε
Strain rate	$\dot{\varepsilon}$
Strain rate sensitivities	m
Yong's modulus	E
Moment of inertial	I
Grain size	r
Misorientation angel driven Grain Rotation Coalescence mechanism	GRC
Rate of Coalescence events of grain	v(r, t)
Severe Plastic Deformation	SPD
Engineering Equation Solver	EES
Time	t
Transmission electron microscopy	TEM
Hall-Petch Relationship	HPR
Reverse Hall-Petch Relationship	RHPR
Transmission electron microscope	TEM
Normal Direction	ND
Transverse Direction	TD
Rolling Direction	RD
Semi major axis length	r_1
Semi minor axis length	r_2
Major axis length	r_3
Equivalent radius length	r
Scanning Electron Microscope	SEM
Atomic Force Microscope	AFM
Condensation Particle Counter	CPC
Scanning Mobility Particle Sizer	SMPS

Nanoparticle Tracking Analysis	NTA
Aerosol Particle Mass Analyser	APM
Electron Backscatter Diffraction	EBD

REPORT FORMAT

This dissertation is made up of five major chapters. The first chapter introduces the research project and the general background knowledge of the research. The second chapter deals with the general literature review of the research project. The third chapter deals with the research design and methodology. The fourth chapter deals with interpretation of results and discussion of the materials properties. The last chapter deals with the conclusion and recommendation of the research.

CHAPTER ONE
INTRODUCTION

1.1 Background:

Nanomaterial is a class of materials that is currently attracting significant attention. This is due to the fact that nanomaterials have more enhanced properties when compared to conventional materials. But the fundamental definition of nanomaterials is that these are materials whose internal constituent structures such as grains, crystallites, pores, vacancies, dislocations, grain boundaries and so on belong to nanometer range of length scale or their sizes are less than 100 nm at least in one direction. Although this class of materials has been attracting significant attention for some time now, there exist a lot of controversial results about their mechanical properties. Several reasons have been given about the controversies, some of which include variable grain size distributions (i.e. variable mean grain size and grain size dispersion)(Cuenot *et al*, 2004:1, Tengen *et al*, 2009), varying processing routes resulting from either top-down or bottom up approach (Whang ,2011:22), varying shapes of the internal constituents, (Bhadeshia, 2012:1, Tengen, 2011:585), varying sizes of the specimen being tested, varying means of applying strain to the materials or varying strain rates (Tengen, 2012:198) and weather observations are done locally or globally (Vehoff, Yang, Barnoush, Natter, & Hempelmann, 2008:3). With such controversies, it is difficult to compare data from different researchers (Meyer *et al* 2005:427), making the future of nanomaterials, nanoscience and nanotechnology uncertain. It is therefore necessary for scientists and engineers to come up with a clear way of defining and dealing with nanomaterials' mechanical properties.

1.2 Rationale and motivation:

Nanomaterials can be viewed as a collection of atoms and molecules with variation in textures and orientations at regions such as grain boundaries. As such, nanomaterials have been in existence since the creation of mankind. This is because everything on earth is made up of atoms and/or molecules. Nonetheless, Gleiter only defined nanomaterial in the late 1980s (Whang, 2011:1). It is important to note that nanomaterial study is dealt with in all fields of science and engineering i.e. it is interdisciplinary in nature. These reasons make nanomaterials study a vital area of concern (Whang, 2011:1).

In April 2008, the American Society of Mechanical Engineers (ASME) convened a global summit in Washington DC on the future of mechanical engineering that was attended by more than 120 engineering and science leaders from 19 countries representing industries, academic and government. The theme of the summit was to study the evolution of mechanical engineering between the year 2008 to 2028 (Steven Institute, 2008:3). One of the key outcomes from this global summit was the view that nanotechnology will dominate technology in the next 20 years to come.

However we cannot talk of nanotechnologies without looking at nanomaterials, since nanomaterials are the foundation of nanotechnologies. Thus, with the present controversies on the study of nanomaterials' mechanical properties reported by several researchers, one can claim that there is, therefore, a need to come up with a clearer definition of nanomaterials' mechanical properties stemming from the fundamental definition and classification of nanomaterials.

1.3 Problem statement

Although nanomaterials have been attracting significant interest for some time now, there exist a lot of controversial results about their mechanical properties (see fig.1 on some "controversial" or varying results reported by different researchers for nano-copper). This is further aggravated by the fact that the controversies or variations are even observed and reported by the same set of researchers, (Morris, 2010:175, Tengen, 2011:585, Tengen 2012:198). Several convincing and contradictory reasons have been put forward about the controversies, and several approaches have been employed to address these controversies as outlined in the introduction section of this dissertation. These banks of controversial results and convincing reasons justifying the present controversies in nanomaterials' mechanical properties point out that there is a need to come up with a clearly stated rule of processing and modelling nanomaterials such that the same results can be reproduced.

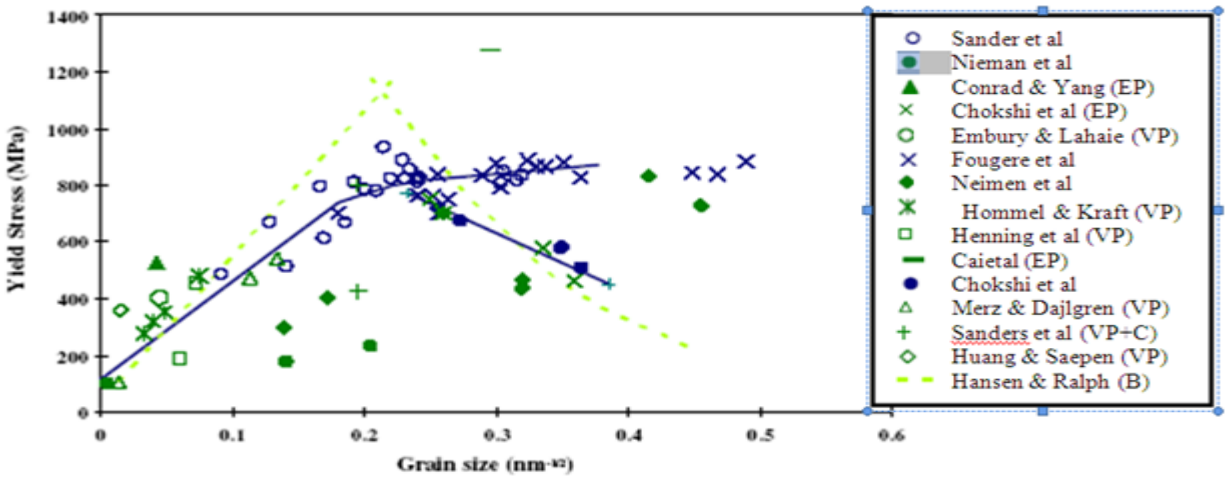

Figure 1: Some "controversial" results reported by different researchers for Cu (Morris, 2010:175)

Recent studies show that, in addition to the impacts of varying methods of imposing strains on materials, the effects of varying definitions of strain (i.e. either true strain or engineering strain), varying definitions of strain-rates and varying definitions of strain rate sensitivities are enormous, (Tengen, 2012:198). Because strain, strain rate and strain rate sensitivity are interconnected, their variable definitions have exponential impacts. Furthermore, the fundamental relationship between nanomaterials' mechanical properties (yield stress) and grain size given as Hall-Petch Relationship (HPR) (Hall, 1951:747 and Petch, 1953:25) have several modifications: first to reveal reverse HPR by Zhao and Jian (2006:472); secondly by Tengen et al (2010:661) to consider the stochastic nature of the nanomaterials constituent structures, etc. Several modifications have

also been done on other characteristics and mechanical properties. For example, the evolution of the grain size during grain growth given by the deterministic Hillert's model (Hillert, 1965:227) has been modified (Tengen et al, 2008:185) to consider the stochastic nature of the grain size.

Thus, this research concentrates on exploring the effects of varying (mathematical) definitions of nanomaterials' mechanical properties, with the aim of finding which definition should be more applicable under given sets of conditions. This is achieved through stochastic mechanics, modelling and experimental verifications of some of the modelled results.

1.4 Research aims:

This research is aimed at ascertaining the acceptable procedure for modelling and design of nanomaterials' mechanical properties. The present study focuses on modelling the evolution of the relationship between nanomaterials' mechanical properties such as yield strength, strain, strain rate, strain rate sensitivities and young's modulus.

1.4.1 Research objective and specific objectives:

The main aim of the present study is to ascertain the correct mathematical definitions of nanomaterials' mechanical properties that are suitable under a given set of conditions to be used for experimentations and modelling. To achieve this, the following are the specific objectives to be dealt with:

1. Identifying relevant models (definitions) for the relationship between nanomaterials' mechanical properties such as yield strength, strain, strain rate, strain rate sensitivities and young's modulus
2. Modify the model's equations so as to confirm this with the theory of stochastic mechanics.
3. Obtain data for the parameters (i.e. material properties) needed to validate the identified and modified models
4. Run the models and obtain the relationships between some of the mentioned mechanical properties.
5. Obtain experimental results or data on some of the mentioned nanomaterials' mechanical properties under a given set of conditions including varying temperature
6. Correlate the stochastic models' results with experimental results so as to ascertain the correct models to be used under the given set of conditions

CHAPTER TWO
LITERATURE REVIEW

2.1 Controversies on Nanomaterials' mechanical Properties.

Presently, there exist a lot of controversies about nanomaterials' mechanical properties (Morris, 2010:175, Tengen, 2011:585 and Tengen, 2012:198). Scientists and engineers are still trying to make a breakthrough in this area of science and engineering, which proves difficult because of the many controversies and convincing reasons justifying the controversies (Morris, 2010:175, Tengen, 2011:585 and Tengen, 2012:198). Some of the reasons given are numerous processing routes, varying processing techniques, varying means of imposing strain on the materials, varying internal constituent structures, varying grain size, varying definition of equations, whether the observations are done locally or globally etc. "*It is therefore very difficult to talk of precision when dealing with nanomaterials' mechanical properties".*

It was reported by Estrin & Vinogradov (2013:782) that the various methods of severe plastic deformation (SPD) have their advantages and their limitations. The difference between the various SPD methods lies in the mode of deformation of the specimen, in regards to the way of imposing strain to the specimen. The SPD is based on a top-down approach, which naturally has an advantage over a bottom up approach, because the SPD fabrication is free from porosity, vacancy, and dislocations that are common in a bottom-up approach and the possibility of obtaining several strain data is also prominent of the SPD approach. The various techniques of producing nanomaterials and their effects on the physical and mechanical properties have shown that the SPD method is the most widely used method to impose high strain to a bulk solid (Estrin & Vinogradov 2013:790). Temperature has been reported (Estrin & Vinogradov, 2013:1) to have a significant effect on grain sizes, as well as the strength of the materials. The phenomenon leading to this conclusion is referred to as thermo-mechanical processes (Estrin & Vinogradov, 2013:1).

2.2 Considering Temperature during Modelling of nanomaterials' mechanical properties.

Temperature has a vital role to play during grain refinement since all SPD techniques involve thermo-mechanical processes. Kumar (Kumar & Sharma, 2013:5) reported that the thermodynamic properties of nanomaterials depend on their vibration energy. Kumar (Kumar et al. 2013:5) developed a theoretical model and studied the effect of temperature on properties. Kumar (Kumar et al. 2013:5) compared theoretical results with experimental results. Similarly, Guisbiers (Guisbier. 2010:1132) also developed a model predicting the dependence of melting and cohesive energy of nanocrystalline materials. Guisbiers (Guisbier. 2010:1132) compared obtained results with different models' results. Zhang (Zhang et al. 1999:249) also demonstrated that, a simple model, free from any adjustable parameters, can be developed for the melting enthalpy and melting entropy of nanocrystals. The idea was based on Mott's equation for the melting enthalpy and melting entropy for non-semiconductor crystals modelling of their melting temperature. The most important

characteristic of materials at nanoscales is their high surface to volume ratio which affects their thermodynamic properties. It is now well known that the melting temperature of nanoparticles impact nanomaterials' mechanical properties (Xiong, Qi, Cheng, Huang, Wang & Li, 2011:10652) since temperature plays a vital role in material properties (Estrin et al. 2013:1).

Material yield stress (σ_y) and strain rate ($\dot{\varepsilon}$) can be related through a power law (Kreitcberg et al. 2014:1) given by $\sigma_y = K\dot{\varepsilon}^m$ where m is the temperature dependent strain rate sensitivity (SRS) factor. K is a proportionality constant that is being ignored by taking logarithms on both sides of the equation. It was observed that at extremely low temperature the SRS was small and at high temperature the SRS increased and resulted in material hardening. It is shown here that temperature is a key factor during the manufacturing of nanomaterials since temperature influences the mechanical properties of yield stress (σ_y) and strain rate ($\dot{\varepsilon}$) (Kreitcberg et al. 2014:1). Therefore, to ascertain the correct mathematical models of nanomaterials' mechanical properties temperature is a key factor that must be considered.

2.3 Considering Size during Modelling of nanomaterials' mechanical properties.

Materials are called nanomaterial because of their refined grain sizes and enhanced mechanical properties. From the fundamental definition of nanomaterials, size plays an important role in the classification of nanomaterials' mechanical properties. Emil Roduner (2006:1) reported that size plays a vital role in the classification of physical properties in nanomaterials. It was shown that "*different size in nanomaterials during experimentation is one of the reasons for different properties being obtained, since the stress flow or strain being incurred in a material will greatly depend on the size of the material under investigation".*

Studying the stress or strain flow in a material, the bigger the size of the material the lower the stress or strain distribution and the smaller the size of the material the greater the stress or strain distribution. From this observation it can be concluded that the stress or strain distribution in carbon, gold, aluminium, copper, platinum, etc. will greatly depend on how big or how small the material under investigation is when characterizing their mechanical properties. It was also observed that the overall mechanical properties of nanomaterials are quite different due to the random size and shape of the building blocks (or inclusions) whose mean values and dispersions may not be the same (Tengen, 2011:585). It was, however, revealed that size has a vital role to play in designing nanomaterials with desired mechanical properties (Tengen, 2011:585).

Nanomaterials' mechanical properties are given as a function of size (Hofmann, 2011:1, Hillert, 1965:227, Hall, 1951:747, Petch, 1953:25, Zhao et al. 2006:472 and Wang et al. 2008:6). The initial model of size evolution and property was established by Hillert (1965:227). Hall and Petch (Hall, 1951:747 and Petch 1953:25) studied mechanical properties differently namely as a function of grain sizes and arrived at the same conclusion. The Hall-Petch-Relationship (HPR) states that, as the sizes of the grains in the materials get finer, the yield stress increases. This relationship has its shortcomings (or controversies) in that infinite refinement

should lead to infinite yield stress, which is not the case. For decades now, improvement on HPR has been an issue that has called for many investigations. Modification was done on the HPR to reveal the Reverse Hall-Petch Relationship by Zhao et al. (2006:472). The Zhao (Zhao et al. 2006:472) model was modified by Tengen et al (2010:661) to consider the stochastic nature of grain size.

2.4 Modification of 2-D grain models

Several SPD techniques have been developed and tested such as Equal-Channel Angular Pressing (ECAP), High Pressure Torsion (HPT), Cyclic Extrusion Compression (CEC), Accumulative Roll Bonding (ARB) (Lewandowska, 2006:1) and so on. Amongst these techniques the ARB method is unique due to its ability to improve on productivity of bulk nanostructure material during manufacturing. Whang (2011:41) suggested that ARB should be carried out at very high temperature below the recrystallization temperature of the specimen to ensure good bonding. When the ARB is performed at elevated temperature, more often it leads to elongated grains that influence mechanical properties, specifically the formability and workability of a nanocrystalline material (Saito et al. 1998:1221, Tamimi, Ketabehi & Parvin, 2008:2556). In addition to these significant impacts of elongation, the ARB has been adopted by most steel industries because of its mass production ability (Estrin & Vinogradov, 2013:788).

Grain-elongation may be defined as the lengthening of grains into various shapes. It should be recalled that the "true" shape of an inclusion does not depend on location of the cutting plane nor orientation (Tengen, 2011:2). Different shapes and sizes of grain have been reported to have different impacts on the overall properties of the nanomaterial's internal constituent structures (Tengen, 2011:2). Some of the reasons why the characterization of the internal constituent structures and their impacts on the mechanical properties have seen several modifications, are due to the random nature of the internal constituent structures. Some of the modifications or improvements of the internal constituent structures characterization include, firstly, the evolution of the grain size during grain growth given by the deterministic Hillert's model (Hillert, 1965) that has been modified (Tengen et al. 2008:185) to consider the stochastic nature of the grain size. Secondly, the fundamental relationship between the nanomaterials' mechanical properties (yield stress) and grain size given as the classical Hall-Petch Relationship (HPR) (Hall, 1951:747 & Petch, 1953:25) has seen several modification: first to reveal Reverse HPR by Zhao and Jian (2006:472); secondly by Tengen et al (2010:661) to consider the stochastic nature of the nanomaterial's constituent structures.

Most previous findings report on average grain size, average dislocation density and average spacing between boundaries (Tengen, 2011:585). Furthermore, most models directly deal with parameter such as equivalent radius of the elongated grains with the assumption that the grains of nanocrystalline structures are spherical in shape (Tengen, 2011:585).

This research adopts the task of first "*ascertaining the correct mathematical models to be used for experimentation and modelling"*. After thorough literature survey it was observed that size and temperature are two important parameters that must be considered in selecting the relevant mathematical definitions for nanomaterials' mechanical properties. After selecting the relevant mathematical models for nanomaterials' mechanical properties, the models were modified by considering the different direction of observation from the cutting plane which are the normal direction (ND), transverse direction (TD) and rolling direction (RD) or the sliding direction (SD). A grain undergoing SPD by ARB and ECAP have different directions of observation from the cutting plane (direction along the ND, TD and RD or SD) (Segal, 2005:205). The grain orientation along the ND can be observed from the direction along TD and RD, and the grain orientation along the TD can be observed along the ND and RD, and finally the grain orientation along the RD can also be observed along the ND and TD. For the 2-D grain model the grain orientations were observed along the TD and ND whereas for the 3-D grain model the grain orientations were observed along the ND, TD and RD or SD which is a real world problem.

It has generally been reported by researchers that, materials deformed by Accumulative Roll-Bonding and Equal Channel Angular Pressing are generally elongated but none of these researchers have developed a model of elongation (Saito et al. 1998:1221, Tamimi et al., 2008:2556). Elongation gives more information about "size" during grain refinement. The model for grain elongation (William, 1998:9) was modified to be applicable to 2-D grains and 3-D grains. The effects of size on elongation and nanomaterials' mechanical properties were studied.

2.5 Modification of 3-D grain models

Materials are called nanomaterials because of their refined grain sizes. Presently there are controversies when comparing nanomaterials' mechanical properties. The existing controversies have brought confusion in the scientific community. Since several controversies exist, several results have been published. Most recent work on nanomaterials' mechanical properties may not be accepted since new findings are bringing more controversies into the study of nanomaterials' mechanical properties. This research is aimed at showing that most of the published results may be correct, although controversies exist when comparing the different results. This research has shown that different approaches of measuring nanomaterials' mechanical properties may lead to different results being obtained. This is an indication that researchers considered different approaches of measuring nanomaterials' mechanical properties which has resulted in different results being obtained. This dissertation revealed more properties of nanomaterials that may be ignored by considering only the measurement as the equivalent radius. Most of the new findings on nanomaterials' mechanical properties may have been rejected although they expose results which may be of great value since different approaches have been undertaken in this research.

The sizes of 3-D grains can be described by the equivalent radius r, semi major axis length r_1 semi minor axis length r_2, and major axis length r_3. Most models for grain size evolutions are given as a function of spherical grains (Hall, 1951:747 & Petch, 1953:25) although with random size distribution. Most of these existing models of nanomaterials' mechanical properties dealt only with the equivalent radius r or made the assumptions that the grains in nanomaterials are spherical in nature (Hall, 1951:747, Petch, 1953:25, Hillert, 1965:227, Tengen, 2008:20, Zhao et al. 2006:472 & Tengen et al 2010:661).

Experimentally, it was shown that this assumption of a spherical shape of all the grains in nanomaterials is not the case. In fact, the majority of the grains in nanomaterials are not nearly spherical in nature. Thus, these existing models, which consider that the grains in nanomaterials are spherical, ignore other important parameters such as semi-minor axis length r_2, semi-major axis length r_1 and the major axis length r_3, which can be used to closely define grain elongation and shape. It must be remarked here that a grain undergoing elongation during nanomaterial refinement might not change in equivalent radius (with equivalent radius defined as the radius of an equivalent sphere or circle obtained by the displacement method of volume/area measurement). As such, the impacts of grain elongation on nanomaterials' mechanical properties cannot be properly addressed with the use of equivalent radius only.

Transmission electron microscopy (TEM) revealed different approaches of measuring grain size variants, that are different parameters which most developed models that dealt only with the equivalent radius ignored (Hidalgo, Cepeda, Ruano & Carreno 2012: 287 & Cai, Bellon, 2013 :602). The TEM revealed that grains deformed by severe plastic deformation (SPD), specifically the accumulative roll-bonding (ARB) and equal channel angular pressing (ECAP), has three main directions of observation. The observation directions are the normal direction (ND), transverse direction (TD) and the rolling direction (RD) or sliding direction (SD) as shown in Fig.2. Thus the use of the equivalent radius only, cannot give more information about the shape of a grain during grain refinement since the TEM have revealed other approaches of measuring grain size during grain refinement.

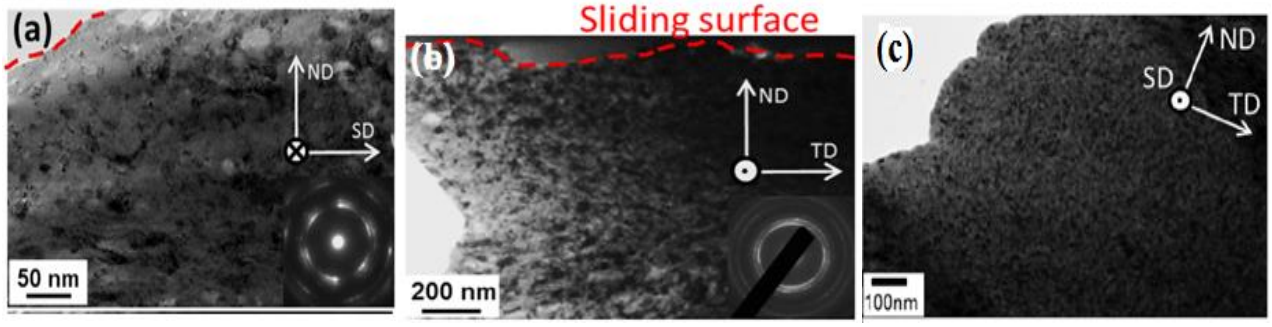

Fig.2: Dark-Field TEM microstructural and crystallographic and texture evolution revealing different approaches of measuring grain sizes property along TD, ND and RD or (SD) revealed by (Cai et al., 2013 :602).

Segal (Segal, 2005:205) reported that the subsequent flow mechanism depends on the deformation mode which has a strong effect on textural (geometrical) hardening. It has also been reported that a grain undergoing SPD by ARB and ECAP can be observed from different directions depending on the orientation of the cutting plane (direction along the ND, TD and RD or SD) (Segal, 2005:205). The grain orientation along the ND can be observed from the direction along TD and RD, and the grain orientation along the TD can be observed along the ND and RD, and finally the grain orientation along the RD can also be observed along the ND and TD.

Segal (Segal, 2005:205) observed a stable crystallographic orientation at the original position, after pure shear and after simple shear in the study of deformation mode and plastic flow in ultra-fine grained metals. Segal (Segal, 2005:205) revealed that the subsequent flow mechanism depends on the deformation mode which has a strong effect on textural (geometrical) hardening. Segal (Segal, 2005:205) presents a model for evolution of originally near random texture under pure shear and simple shear with different directions of grain orientation. From Segal's (Segal, 2005:205) study of grain orientation during grain refinement, it has also been revealed that varying grain sizes exist with varying grain angles during grain refinement. It is therefore clear that the existing models that consider only the equivalent radius during grain refinement ignored other approaches of quantifying or modelling nanomaterials' mechanical properties. In this research, the measurement of grain size along the TD is represented in the model as the semi major axis length r_1, the ND is represented in the model as the semi minor axis length r_2, and the RD or SD it is represented in the model as the major axis length r_3.

2.6 Methods of Measuring and Characterizing Nanomaterials' mechanical/Physiochemical Properties.

Scanning Electron Microscopy (SEM)

The Scanning electron microscope (SEM) is a microscope that can give images of a material by scanning the material with a special beam of electrons (Arenas, Silva, Alva, Rivera, 2009:617). During the scanning process the electrons interact with the atoms of the sample to produce the needed signals that contain information about the sample (Arenas et al., 2009:617). Some of the advantages of the SEM is that samples used for SEM study need minimal sample preparation (Arenas et al., 2009:617). However, the disadvantages of SEM are its cost and size (Arenas et al., 2009:617). SEM is very expensive and it must be kept in an area free of any possible electric, magnetic or vibration interference (Arenas et al., 2009:617). Proper maintenance of the SEM is usually expensive (Arenas et al., 2009:617). Special tutorials and training is needed to operate the SEM. It is not always easy to use the SEM, since it carries a small risk of radiation from beneath the sample surface (Arenas et al., 2009:617). SEM users and researchers are advised to observe safety precautions due to the chance of radiation escaping the chamber (Arenas et al., 2009:617).

X-ray Diffraction

X-ray diffraction are usually caused by the interference of constructive scattered waves (Hil, 1956:1). The x-ray diffraction can actually perform qualitative and quantitative analysis of nanocrystalline materials. It has variations and different operation which are used for quantitative and quantitative studies (Hil, 1956:1). It has the following advantages: The diffracted beams of x-ray diffraction have a high intensity (Hil, 1956:1). The orientation of the crystal along the direction can be easily achieved (Hil, 1956:1). The diffraction patterns of the sample can be observed or obtained from samples with crystals selected with a diffracted aperture (Hil, 1956:1). However, its disadvantage is that the intensities of the reflections are highly influenced by dynamical effects (Hil, 1956:1).

Atomic Force Microscopy (AFM) or Scanning Force Microscopy (SFM)

AFM is a very high resolution microscopy process which has the ability to demonstrate resolution of fractions of a nanometre (Arenas et al., 2009:617). It has major abilities such as manipulation, imaging and force measurement. The AFM is designed to measure height, fraction, and magnetism on the sample (Arenas et al., 2009:617). Advantages of AFM is that the sample being examined does not need special treatment such as carbon coatings such as is the case for SEM (Arenas et al., 2009:617). AFM gives higher resolution than SEM (Arenas et al., 2009:617). However, the disadvantages of AFM is that its images can be affected by nonlinearity (Arenas et al., 2009:617). AFM cannot easily measure steep walls or overhangs in the structure. (Arenas et al., 2009:617)

Condensation Particle Counter (CPC)

The Condensation Particle Counter is an instrument that actually detects and counts particles (Hermann, Birgit, Oliver, Han, Thomas, Liu, 2007:674) one at a time (Hermann et al., 2007:674). It has a high light intensity source that illuminates the particles as the particles pass through the direction chamber (Hermann et al., 2007:674). The advantage of the CPC is its uniqueness to detect and counts very small particles (Hermann et al., 2007:674).

Differential Mobility Analyser

The differential mobility analyser is an instrument that separates the changed aerosol particles due to the mobility in the electric field (Chen, Schwegler-Berry, Cumpston, Cumpston, Friend, stone & Keane, 2016:501). The differential mobility analyser can measure submicron aerosol size distributions. It also measures much smaller particles of about 2.5nm (Chen et al., 2016:501). It is also very sensitive to differences in refractive index and also sensitive to variations in the shape of the particle (Chen et al., 2016:501).

Scanning Mobility Particle Sizer (SMPS)

The SMPS is an analytical device that measures the size and the concentration of aerosol particles with diameters ranging from 2.5nm to 1000nm (Chen et al., 2016:501). It has an advantage in that it provides a continuous fast scanning technique which gives a high resolution measurement (Chen et al., 2016:501). It also has little information on its performance in analysing full spectrum of nanoparticles (Chen et al., 2016:501).

Nanoparticle Tracking Analysis (NTA)

Nanoparticle Tracking Analysis (NTA) is mostly used for analysing and visualizing particles in liquids. The rate of movement of the particles is related to viscosity and temperature of the liquid. However, the movement of the particle is not influenced by density or refractive index. Its advantage is that it has a very high intensity of scattered light which is used to detect small amounts of large particles. Its main disadvantage is that dust or small amounts of large aggregates has an effect in determining the size of the nanoparticles (Vasco, Andrea, & Wim, 2010:796).

Aerosol Particle Mass Analyser (APM)

APM is a technique used for measuring and classifying aerosol particles according to their mass-to-charge ratio. It does not depend on gas properties such as temperature, viscosity and pressure. There is no semi-empirical corrections such as a slip correction factor. The system can be calibrated during the measurement. Its main disadvantage is that gravimetric filter measurements can lead to sampling artefacts (Jonathan, Kingsley, Jason, 2013:47).

Ultraviolet-visible spectroscopy (UV-vis spectra)

The UV-vis spectroscopy uses visible and adjacent light. Main drawback is the failure to give absorption data for wavelengths below 200nm (Masayoshi, 2002:108).

Electron Backscatter Diffraction (EBD)

The electron backscatter diffraction (EBD) is a technique which is used to characterize the microstructures of polycrystalline materials. It gives the structure, crystallographic orientation and different phases of the deformed materials. It is mostly used to explore microstructures of deformed materials since it reveals the texture, defects, grain morphology and deformation of the microstructures. However, its main drawback is the high cost of its image intensified video camera system (Barr, Brown, 1995:66).

The used of TEM in this Study and the Justification

Transmission electron microscopy (TEM) is a microscopic technique in which a beam of electrons is transmitted through an ultra-thin specimen, the interaction of electrons transmitted through the ultra-thin specimen produces an image (Hidalgo et al., 2013:602-610) (Arenas et al., 2009:617). The produced image is magnified by a fluorescent screen on a layer of photographic film (Hidalgo et al., 2013:602-610). The TEM has the ability of imaging at higher resolution than other light microscopes (Hidalgo et al., 2013:602-610). The significantly higher resolution in the TEM gives more advantages for the operator to examine fine detail - even as small as the size of single atoms (Hidalgo et al., 2013:602-610) (Arenas et al., 2009:617). Therefore, the TEM can actually measure thousands of time smaller than smallest atoms which other light microscope cannot measure (Hidalgo et al., 2013:602-610) (Arenas et al., 2009:617).

The TEM forms a major analysis method in most scientific fields and in most industrial applications. The TEM is the most powerful microscope (Hidalgo et al., 2013:602-610). It could be seen that the TEM offers the most enhanced magnification of all microscopes (Arenas et al., 2009:617). The TEM images are of high-quality and contain more details than images of other microscopes (Hidalgo et al., 2013:602-610). The TEM can actually give more information of surface features, shape, size and structure which this dissertation used in the derivation of models (Hidalgo et al., 2013:602-610). More importantly, it is easy to operate a TEM after proper training. These are the main reason why this study focused on the utilisation of the TEM.

2.7 The Strain Rate Sensitivity (SRS) Models

The strain rate sensitivity (SRS) is important in determining the deformation mechanisms of nanostructured materials (Vasin et al. 1997:1, Jiao Luo et al. 2009:741 & Kreitcberg et al. 2014:1). Several studies on SRS have been carried out and these have contributed to the present controversies on nanomaterials' mechanical properties. The varying definitions of model equations of SRS, contribute greatly to the present controversies on nanomaterials' mechanical properties (Jiao Luo et al. 2009:741). Since nanomaterials' constituent structure characteristics are random in nature, with random spatial distribution, these characteristics can be modelled with the tools of stochastic mechanics (specifically stochastic processes), which deal with field variables that have the ability to model random spatial patterns (Tengen, 2011:1). Furthermore, since the present study focuses on modelling the relationship between nanomaterials' mechanical properties, the research project is designed as follows: identification and possible modification of model equations followed by experimentations and validation of essential models. The different methods and techniques to compute SRS are explained below.

A. The Methods of Tensile Test

During this technique a jump test were conducted using a universal testing machine by varying the strain rates by 10 % for every 100% increment of elongation (Anton et al. 2009:389). The SRS values for various strains were computed using the expression (Anton et al. 2009:389).

$$SRS = \frac{\log\left(\frac{\sigma_2}{\sigma_1}\right)}{\log\left(\frac{\dot{\varepsilon}_2}{\dot{\varepsilon}_1}\right)} = \frac{\log \frac{F_2}{F_1}}{\log \frac{V_2}{V_1}} \quad (2\text{-}1)$$

where σ_1 and σ_2 are the flow stresses corresponding to instantaneous strain rates ε_1 and ε_2 . F_1 and F_2 are the forces and V_1 and V_2 are the cross-head speeds before and after the jump.

The SRS values at a single strain was calculated, at a fixed strain rate using the experimental data of the cross-head speeds V_1 and V_2 with the corresponding forces F_1 and F_2. A series of SRS values were computed from the jump test and plotted as a function of strain rates. The SRS was measured at different temperatures in the strain rate jump tensile test.

B. The Compression and Vishay Micro Measurement Techniques

Sabirov et al., (2009:679) studied the relationship between SRS of the flow stress and the operative deformation mechanisms in the ultra-fine grain (UFG) Al–Mg–Si (Al6082) alloy under compression. Their results of compression testing revealed that increased SRS due to grain boundary sliding and micro shear banding, offers enhanced ductility at low strain rates. Another study on SRS by Brand et al., (2007:1) revealed that the SRS can be calculated by measuring the strain. It was, however, observed that at high deformation temperature, the SRS increased with increasing deformation temperature (Jiao Luo et al., 2009:741, May et al., 2005:189 & Meyers et al., 2006:427). Several studies have shown that nanomaterials are very sensitive to temperature (Jiao Luo et al., 2009:741, May et al. 2005:191, Meyers et al. 2006:507, Lee et al., 2008:336 & Chiou et al. 2009:94). Varying temperature during deformation of conventional materials to nanostructured materials affects the SRS of materials (Jiao Luo et al., 2009:741).

Another most important characteristic of materials at nanoscales, is their high surface to volume ratio which affects their thermodynamic properties and SRS (Zhang et al. 1999:249). It is well known that the melting temperature of nanoparticles depends on their size (Xiong et al. 2011:10652), thus, size and temperature are important parameters when studying nanomaterials' mechanical properties. Although the size-dependent properties are so useful, a unique attempt to establish a quantitative model describing the size dependence of SRS, based on the simple consideration of surface/volume ratio, cannot satisfactorily interpret the stochastic nature of grain size. Thus, it is necessary to model the grain size quantitatively into grain size variants (3-D grain). *In this research, the SRS is computed on grain size variants and the effect of processing temperature on SRS are discussed based on a 3-D grain deformed by Accumulative Roll-Bonding (ARB) and Equal Channel Angular Pressing (ECAP).*

2.8 The Deformation Activation Volume and Strain Rate Sensitivity (SRS) Models

The micro-mechanisms of size dependent strengthening are commonly explained by the dislocation starvation effect application at nanoscale (Wang, Shan, Sun & Ma. 2012:1 and Zhou, Beyerlein & Lesar. 2011:7673). High strain rate sensitivity (SRS) and low activation volume has been observed by Zhu, Li, Samanta, Leache, & Gall. (2008:1). Although nanoscale materials are being considered for different applications due to their enhanced mechanical properties, their rate limiting processes of activation volume remain a "lack of deep understanding" that has called for many investigations (Zhu et al., 2008:1). Most researchers have demonstrated the relationship between SRS and activation volume without considering the grain size variants on the activation volume (Anton et al. 2009:389) (Sabirov et al. 2009:181) (Abirov, Brad et al. 2007:1). Most recent findings on the relationship between SRS and activation volume are studied on the equivalent radius of the grain during grain refinement (with the equivalent radius defined as the radius of an equivalent sphere or cycle obtained by the displacement method of volume/area measurement). It is therefore, necessary to model the activation volume qualitatively as a function of grain size variants during grain refinement. However, the models of activation volume that dealt only with the equivalent radius, ignored other approaches of measurement during grain refinement. In this research, the effect of processing temperature on the activation volume and grain size for 3-D grains that are deformed by Accumulative Roll-Bonding (ARB) and Equal Channel Angular Pressing (ECAP) is investigated. The proposed models are tested with data from grain deformation in nanocrystalline aluminium samples.

2.9 Material Flow in Ultra-Fine Grain (UFG) Metals

During grain refinement the size of the grain decreases into the ultrafine regime (Meyer et al., 2005:501). It is also observed that for all smaller grain sizes shear band development is usually observed to occur immediately after plastic deformation (Meyer et al., 2005:503). Meyer et al., (2005:503) and other researchers observed shear bands in both low and high strain rates tests. The development of shear bands in quasi-static deformation increased with increasing strain. The shear bands formed during grain deformation produced equiaxed grains with relatively low dislocation density, which Meyer et al., (2005:503) reported as being due to dynamic recrystallization. Segal (2005:205) reported that ultra-fine grained (UFG) materials produced by SPD, show many unusual properties and that their plastic flow defines their strength, ductility, toughness, fatigue and other characteristics. Segal (Segal, 2005:205) reported that the flow mechanism in a material depends on the deformation mode which has a strong effect on textural (geometrical) hardening of the material during grain refinement. The material flow in ultra-fine metals deformed by ARB and ECAP have different material flow patterns along the ND, TD and RD or SD during grain refinement.

2.10 Grain Refinement in Ultra-Fine Metals

Grain refinement is the process by which the average grain size in a polycrystalline material decreases over time. Grain refinement may be achieved by SPD through the deformation mechanisms of coarse-grained materials which results to recrystallization. The fine grain size or new mechanism may appear since high stresses are required for conventional dislocation mechanisms. Continuous suppression of grain coarsening led to GB segregation (Limin et al., 2012-41). This suppression of coarsening of nano-sized grains at high temperature led to high density of GBs. Material properties enhancement during grain refinement can be explained either through one of the following mechanism.

(a) Grain Boundary Migration (GBM) (Hillert, 1965:227).

(b) Grain Rotation Coalescence (GRC) (Haslam et al., 2001:15).

(c) Grain Breakage Rotation (GBR) Mechanism

(d) A process which involves GBM and GRC (Tengen, 2009:661).

Any of these processes may lead to grain elongation, but the creation of high angle boundaries by grain subdivision is the main activities that led to grain elongation.

"Despite the great interest in SPD during past years, these deformation mechanisms are still uncertain (Segal, 2005:205). Research work with various SPD techniques and conditions gives different models for developed high angle boundaries (HABs) and structure refinement (Segal, 2005:205)". Some of the developed models extend the continuous evolution of dislocation structures by the crystallography glide from low and moderate strains SPD. An alternative method describes the SPD as discontinuous due to localized flow inside shear bands (SBs) of non-crystallographic orientations (Segal, 2005:205).

Segal's original contributions provoked the scientific community to study the microstructure of a material that was deformed by SPD (Laszlo et al., 2014:1). The most important characteristic of microstructure is grain size and the ultrafine grain structures are normally developed by SPD (Laszlo et al., 2014:1). It is observed that the ECAP process is not continuous; this is why the High Pressure Torsion test (HPT) was introduced to permit extremely large strain in a single operation. Extreme plastic straining led to distorted structures where the grain boundaries are in an "unstable" state. At this state the grain boundaries are characterized by more grain boundary energy, enhanced free volume and the presence of long range elastic stresses (Laszlo et al., 2014:1) during grain refinement.

Grain refinement is caused by dislocation accumulation and rearrangement of material with medium to high stacking fault (SF) energy. Wang (Wang, Ho, Li, Ringer & Zhu, 2009:1) reported that Twining also plays a key role in grain refinement. Wang et al., (2009:1) also reported that there is always a minimum average grain size that a specific SPD condition can achieve for a specific material and this minimum size is a function of not only the intrinsic material properties such as SF energy but also the extrinsic processing parameters. It was also reported by Wang et al., (2009:1) that when this minimum grain size is produced during SPD processing it also results in grain growth. The minimum grain size is achieved by the dynamic balance between the grain refinement process and the grain growth process (Wang et al., 2009:1).

Severe plastic deformation induced grain growth has been widely reported in various plastic deformation techniques including nano-indentation, high pressure torsion, uniaxial tension and uniaxial compression (Wang et al., 2009:1). The grain growth changes the structures of nanocrystalline materials and therefore affects their mechanical properties (Wang et al., 2009:1). Molecular dynamics simulations and theoretical analysis have been carried out to understand the mechanisms of deformation inducing grain growth, and *contradictory* results have been reported (Wang et al., 2009:1).

2.11 Grain Rotation and Coalescence (GRC)

Grain rotation and coalescence process takes place when grains rotate and join as a single grain. It brings about a change in the size of a grain at any instant when the misorientation angle between some adjacent grains becomes zero (Tengen, 2012:198) (Haslam, Moldovan, Phillpot, Wolf and Gleiter, 2001:15). The time evolution process shows grain rotation of grain A towards grain B and coalescence with grain B resulting in elongated grain A-B as shown in Figure 3 (a-b) (Haslam et al., 2001:22). In the initial configuration the two grains are disoriented by approximately 18^0 (Haslam et al., 2001:22). During the initial deformation grain A, B and C shrink due to GB migration, while grain B has already undergone some significant rotation towards the orientation of grain A (Haslam et al., 2001:22). It is further observed that grain B, has actually grown again due to continuous rotation (Haslam et al., 2001). It is also important to know that the inclination of GB migration between grains A and B has changed during this process. Finally the coalescence of grains A and B is observed in Figure 3(b) where two grains now being closely aligned with low-angle GB between them was reduced to single dislocation (Haslam et al., 2001:22).

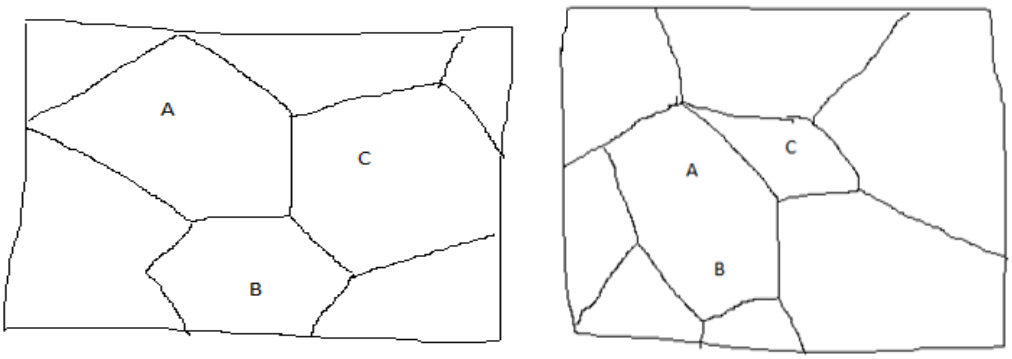

(a) **(b)**

Figure.3. Grain Rotation Processes (Haslam et al. 2001:22).

Figure 4 (a) is a complementary view of grain rotation-coalescence mechanism (Haslam et al., 2001:19). The diagram in Figure 3 (b) revealed that rotation-coalescence may be seen as "unzipping" of the GB between the two grains with larger angle approximately 18^0 and high concentration of miscoordination in the GB between grain A and B (Haslam et al., 2001:19). Figure 3 (a-b) showing a very high concentration of miscoordination in the GB between grains A and B after a very short period. It is observed in Figure 4 (a) that the misorientation

angle has reduced to approximately 16.5^0 with the creation of a dislocation structure of the GB. Three well separated GB dislocations can be observed in Figure 4 (a) and after a short period of time the misorientation angle decreased to about 9^0 and the dislocations left are shown in Figure 4 (b). The change in inclination of the GB between grains A and B observed in Figure 4 (c) and Figure 4 (d) coincides with this absorption. With the low remaining misorientation angle of about 4^0 after a short period of time as shown in Figure 4 (d) only the dislocation at the centre of the GB remains.

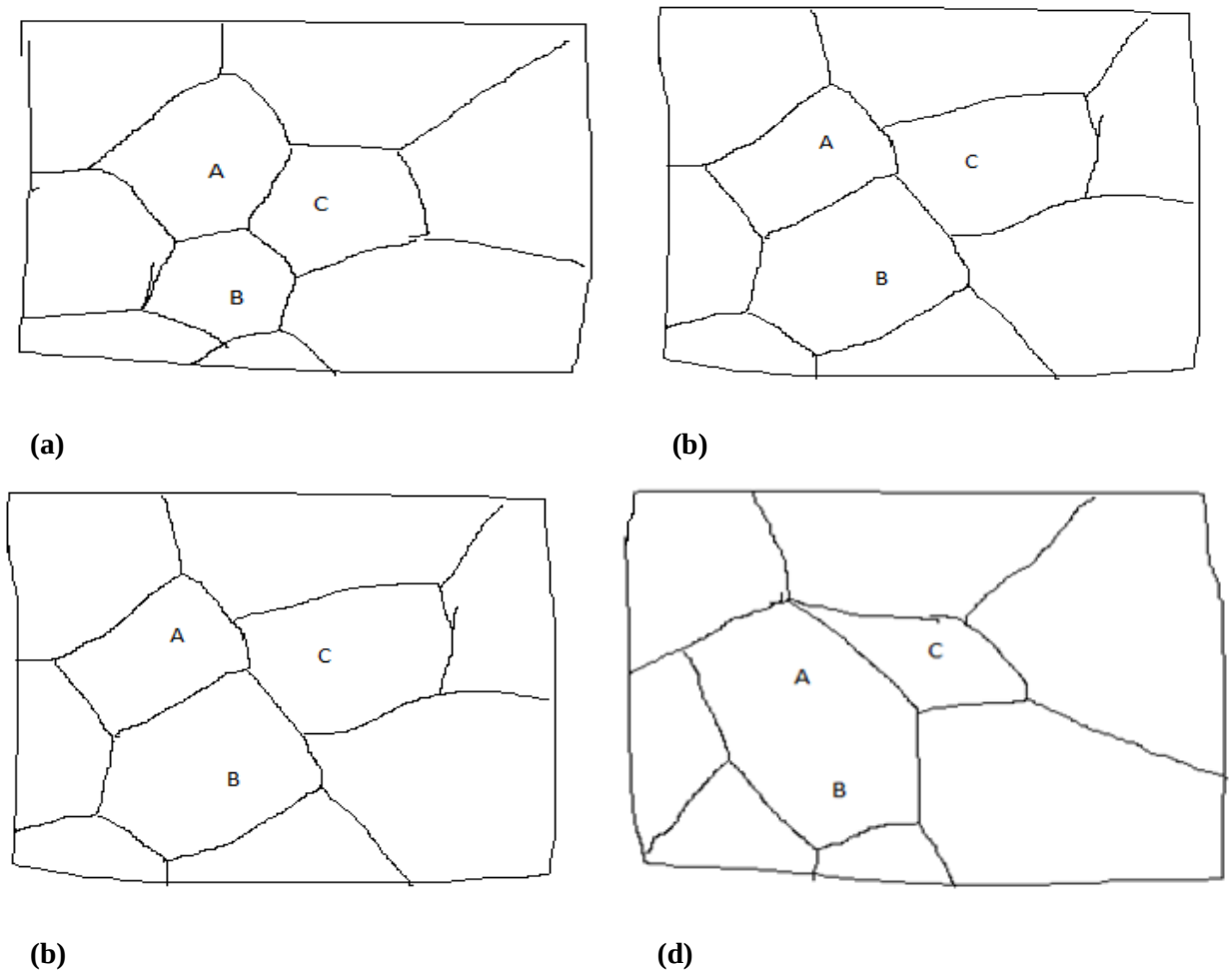

Figure.4. Grain Rotation Processes and Coalescence (Haslam et al., 2001:22).

2.12 Grain-Boundary Based Description of Grain Growth

The force law governing GB migration and GR is given by Newton's law of motion coupling the acceleration of the atoms to the force acting on them (Haslam et al., 2001:22). A constant driving force for migration, p results in a constant drift velocity given by $v = mp$ (Haslam et al., 2001:22) where m is the GB mobility, which is a parameter such as the GB energy and it depends on the GB misorientation and the crystallographic orientation of the GB plane (Haslam et al., 2001:22). From the viscous force law $v = mp$ the mobility is independent of both the driving force and the mechanism of GB migration (Haslam et al., 2001:22). Since the applied force is at an angle, the mobility can be expressed with a force law which is similar to angular velocity

of a rotating grain, ω with respect to an axis through its centre of mass $\omega = \mathrm{M}\tau$ (Haslam et al., 2001:22) where M is the rotational mobility of the grain subjected to a torque τ.

It is reported that some grains experience a net torque for rotation, provided that the total GB energy across all the surface of the neighbouring grains decreases as a result of the rotation (Haslam et al., 2001:22). The rotational mobility of a non-spherical grain embedded in a more or less rigid matrix of all the surrounding grains is strongly influenced by its shape (Haslam et al., 2001:22). The rotation of such a grain necessitates a continuous accommodation process (Haslam et al., 2001:22). Two accommodation mechanisms based on GB diffusion or dislocation motion exist (Haslam et al., 2001:22). At high temperatures the diffusion-accommodation process is more acceptable assuming a hexagonal grain shape within a columnar microstructure and diffusion acts as the accommodation mechanism (Haslam et al., 2001:22).

CHAPTER THREE
RESEARCH DESIGN AND METHODOLOGY

3. A .1.1 Research Design and Methodology

Since nanomaterials constituent structure characteristics are random in nature, with random spatial distribution, these characteristics can be modelled by the tools of stochastic mechanics (specifically stochastic processes), which deal with field variables that have the ability to model random spatial pattern (Tengen, 2011:1). Furthermore, since the present study focused on modelling the relationship between nanomaterials' mechanical properties, it is designed as follows: identification and possible modification of model equations, experimentations and validation of essential models.

The TEM observations indicate that there exist different approaches of measuring nanomaterials' mechanical properties which most previous models on nanomaterials' mechanical properties did not take into consideration. The TEM observation indicates that properties of nanomaterials can be measured in three directions, the ND, RD and TD. Most developed models dealt only with the equivalent radius measurement of nanomaterials' mechanical properties ignoring other approaches of measuring nanomaterials' mechanical properties as revealed by the TEM. The equivalent radius measurement cannot give all the information about a grain undergoing SPD since the equivalent radius measurement ignored other approaches of measuring nanomaterials' mechanical properties as revealed by the TEM.

Grains undergoing SPD, specifically ARB and ECAP, has different directions of observation based on the orientation of the cutting plane (direction along the ND, RD and TD) (Segal, 2005:205). The grains oriented along the ND can be observed from the direction along the TD and RD, and the grain oriented along the TD can be observed along the ND and RD, and the grain oriented along the RD can be observed along the TD and ND (Segal, 2005:205) In this dissertation previous models are modified by considering the different approaches of measuring nanomaterials' mechanical properties as revealed by the TEM (i.e. directions along the ND, RD and TD).

3. A.1.2 Identification and Possible modification of Model Equations

Each mathematical model has its associated parameters, which can be measured differently. For example, if a force F were applied as a pressure P on a cross-sectional area A of a material of mass m such that it moves with an acceleration a, then the force can be measured in two different ways: either by measuring the mass and acceleration of the body and using Newton's Second Law to obtain force from $F=ma$ or by measuring pressure and area on which the force acts to obtain $F=P/A$. Both relationships give the force value, but it can be seen that, the measured parameters are different. Of course, density may be defined as volume-density, area- or surface-density, linear-density or spatial density. It can be seen from various units of these densities that they

can be measured through several techniques. What would one say about unit-less quantities like strain, strain rate sensitivity and so on?

Most models of nanomaterials deal with averages e.g. average grain size, average yield stress, average strain, average grain density, average porosity, etc. (Hall, 1951:747) (Petch, 1953:25) (Hillert, 1965:227) (Tengen, 2008:20) (Zhao et al., 2006:472) and (Tengen et al., 2010:661). But nanomaterial constituent structures are random in nature, it is imperative that those models should be modified to reflect or describe the correct statistical distribution commensurate with the theory of stochastic mechanics. Since models of nanomaterials' mechanical properties mostly depict the relationship between "variables" or characteristics and properties and there are a vast amount of models or properties, only some of the models are considered in this dissertation.

The first model identified from the literature survey was the model of yield stress by Zhao (Zhao et al., 2006:472). The Zhao (Zhao et al., 2006:472) model gives the relationship between yield stress and grain size that depicts HPR to RHPR given as

$$\sigma(r) = \sigma_0^{'} + A\left(r^{-\frac{1}{2}}\right) - B\left(r^{-1}\right) - C\left(r^{-\frac{3}{2}}\right) \tag{3.1}$$

where $\sigma_0^{'} = \sigma_0 + K_t$ is bulk yield stress, $A = K_d$ is HPR proportionality constant, $B = K_t\left[2hH_m / RT_r\right]$, $C = K_d\left[2hH_m / RT_r\right]$, K_t is a constant, h is atomic diameter in the case of metal, H_m is the bulk melting enthalpy, R is ideal gas constant, T_r is the room temperature, $K_d > 100K_t$ and $\sigma_0 > 10K_t$.

The second model identified was the model of SRS which relates material yield stress $(\sigma(r))$ and strain rate $(\dot{\varepsilon})$ as giving by (Anton et al., 2009:389) and (Kreitcberg et al., 2014:1) as

$$m = \frac{\log\left(\sigma_y\right)}{\log\left(\varepsilon^{'}\right)} \tag{3.2}$$

where σ_y is the yield stress and ε' is the strain rate

The third model identified in this research during literature survey was the model of young's modulus given by Wang (Wang et al., 2008:6) as

$$E = \left(\frac{P}{d}\right)\left(\frac{r^3}{192I}\right) \tag{3.3}$$

where the moment of initial is $I = \frac{\Pi D^4}{64}$, $D = r_1$, P is the applied force and d = dr = (r-r_0).

SECTION 3. A. 2

The derived models in this research are based on evolution of grain elongation, size and shape during grain refinement. The models of grain elongation for 2-D and 3-D grains were derived. The model of SRS and activation volume were also developed. The derived models were defined under a given set of conditions during grain refinement and also employing the fact that, grain size distribution evolves as lognormal distribution (Tengen & Iwankiewicz, 2009:461).

3. A.2.1Experimental observations needed for models derivations of 2-D and 3-D grain

When the materials were subjected to grain refinement and followed by 2-D microscopic observation, it was observed that the grains became longer along the semi major axis direction whose length is r_1 and shorter in the semi minor axis direction whose length is r_2 (as shown in Fig.5 (c & d), meanwhile the equivalent radius r decreased. For 3-D microscopic observations, it was observed that the semi major axis length r_1 and major axis length r_3 initially increased (as shown in Fig.5 (g)) and then decreased since grain breakages took place in these directions. As a result of this repeated lengthening and grain breakage processes the effective lengths of r_1 and r_3 decreased during grain refinement. It was also observed during grain refinement that the equivalent axis radius r and semi minor axis length r_2 decrease continuously. It was further observed that r_2 and r_3 were evolved as proportions or fractions of r and r_1 respectively.

3. A.2.2 Models Derivation of 2-D and 3-D Grain

When a sample with a grain of cross section A, initial length r_0 and Young's modulus equal to E is subjected to force (P) due to ARB, the elongation of the grain in 2-D can be obtained from William's model (William, 1998:9) as given by expression (3.4). The model for grain elongation in 2-D (William, 1998:9) can be modified to be applicable to 3-D grains by letting the cross sectional area A be given as $A=V^{2/3}$ as given by expression (3.5). Thus the expression of elongation as defined by William (William, 1998:9) is modified.

$$Elongation = \frac{P\, r_0}{AE} \text{ For 2-D grain} \tag{3.4}$$

$$Elongation = \frac{P r_0}{V^{2/3} E} \text{ For 3-D grain} \quad (3.5)$$

where the expression of young's modulus of nanomaterials is obtained from (Wang et al., 2008:6)

$$E = \left(\frac{P}{d}\right)\left(\frac{r^3}{192I}\right) \quad (3.6)$$

where the moment of inertia is $I = \frac{\pi D^4}{64}$, $D = r_1$ and d = dr = (r-r_0).

Since grain elongation is observed as the lengthening of the grain, it was further observed that the semi minor axis length, semi major axis length, major axis length and equivalent radii varied during grain elongation. At any instant the semi minor axis length, semi major axis length and the major axis length are related to the equivalent radii through equivalent area in 2-D (i.e. through $\pi r_1 r_2 = A = \pi r^2$) and through equivalent volume in 3-D (i.e. through $\left(\frac{4}{3}\right)\pi r^3 = V = (4/3)\pi r_1 r_2 r_3$). This gives

$$r = \sqrt{r_1 r_2} \quad \text{For 2-D grain} \quad (3.7)$$

$$r^3 = r_1 r_2 r_3 \text{ For 3-D grain} \quad (3.8)$$

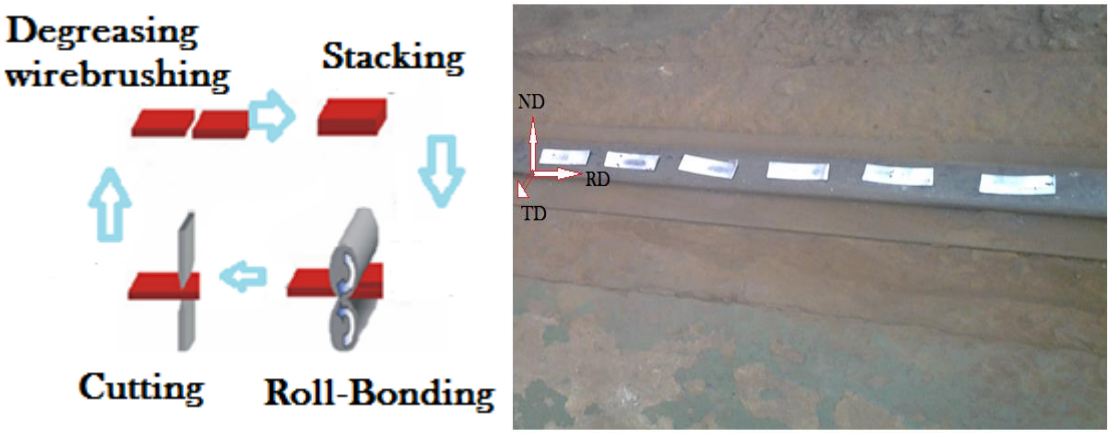

(a) (b)

See figure 5 (a-g) for experimental set up, observation and schematics for model derivation.

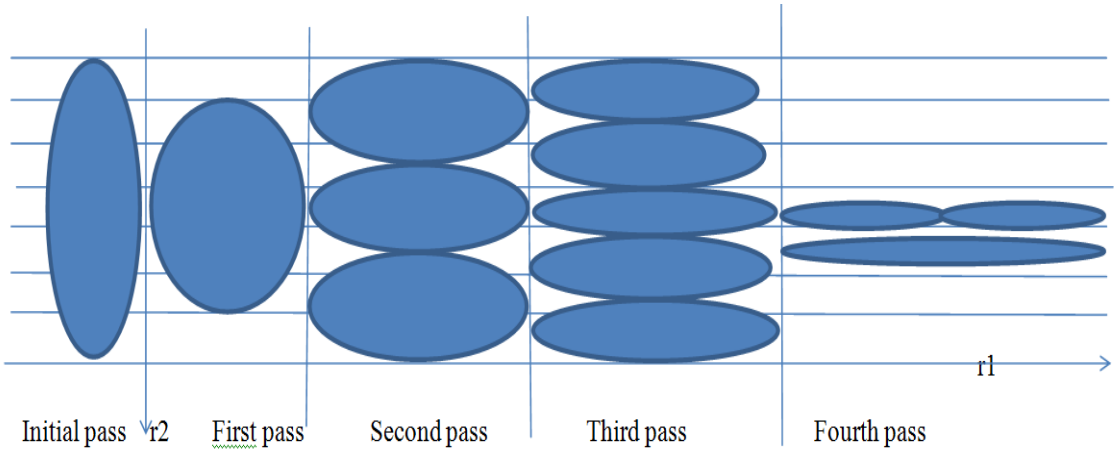

(c)

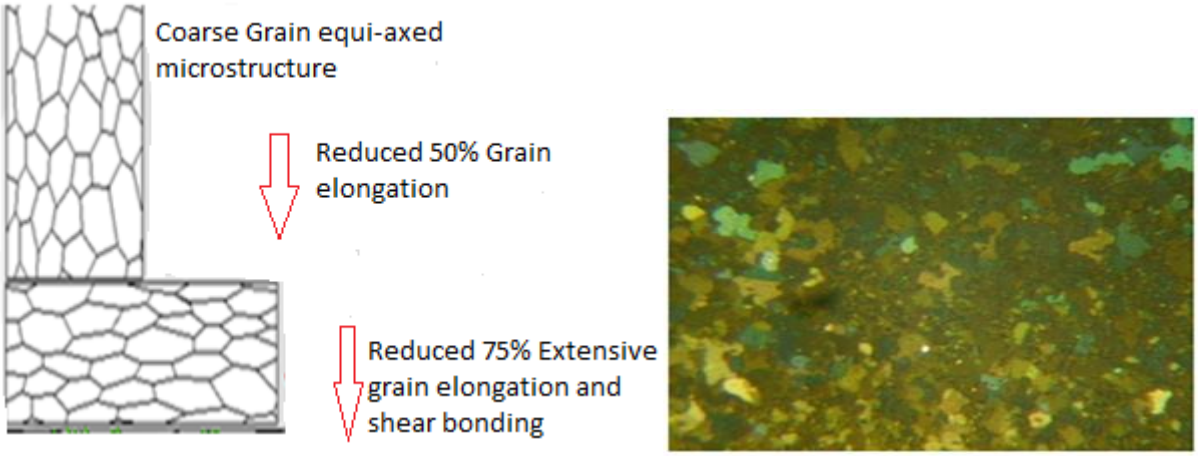

(d) (e)

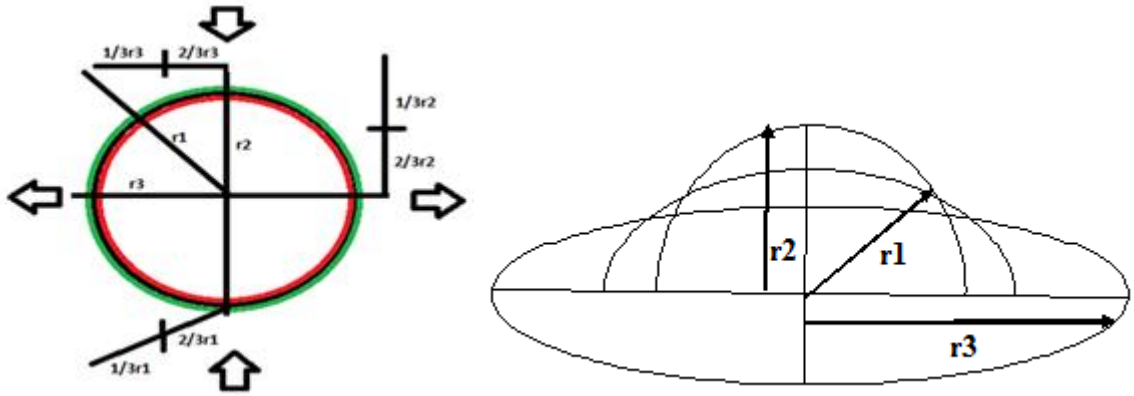

(f) (g)

Figure 5: (a) ARB process (b) deformed materials after ARB cycles (c) Schematic of ARB grain lengthening and grain breakage in 2-D grain (d-e) TEM microstructures (f) Initial grains before deformation in 3-D grain and (g) elongated grains due to deformation in 3-D grain.

It is further observed that the longer grains tend to break along a common grain boundary to form multiple grains. This grain breakage dramatically reduces the lengths of the grains along the semi major axis and the major axis directions, which start to lengthen again. This grain lengthening-and-breakage process repeats itself

over and over leading to the effective lengths of the semi major axis and major axis getting shorter when compared with the starting lengths. It can be said that the evolutions of the semi major lengths and the major axis lengths are stochastic jump processes in nature. Thus, substituting expressions (3.6) and (3.7) into expression (3.4) gives equation (3.9) which is the proposed stochastic model of grain elongation that varies with grain size, r for 2-D grains. Substituting expressions (3.6) and (3.8) into expression (3.5) gives equation (3.10) which is the proposed stochastic model of grain elongation that varies with grain size, r for 3-D grain.

$$Elongation = \frac{3r_0 r_2^3}{r_1^4}\left(r - r_0\right) \quad \text{For 2-D grain} \tag{3.9}$$

$$Elongation = \frac{3\pi r_0 r_1^4}{r_2 r_3 r^3}\left(r - r_0\right) \quad \text{For 3-D grain} \tag{3.10}$$

Since r_1 increased and instantaneously decreased after breakage, the evolution of r_1 during grain refinement can be represented as;

$$dr_1 = M\left(\frac{1}{r_{c1}} - \frac{1}{r_1}\right)dt + r_1^{\frac{1}{2}} DdW(t) - Zr_1 V_1 d(t) \tag{3.12}$$

where $\langle .... \rangle$ = the expected value, r_{c1}=local critical grain size, Z and D are Constants, $dW(t)$=change of the Wiener process, $V_1 = \tau_1 r_1^2$ defines rate of grain breakage, $M = M_0\left(1 + \frac{CD}{r_1}\right)$ is Grain Boundary (GB) mobility function, $CD = 4(Hm)(h_0)/((k)(T)), T_m = T\{ln(m_{01}/m)$ and $M_0 = M_{01}exp\{-T_m(inf)/T\}$= initial grain boundary mobility constant, dW(t) is of wiener process and dN(t) is the number of coalescence events within an infinitesimal time interval.

Since r_3 decreases as a fraction or proportion of r_1 during grain refinement, r_3 can be represented

$$dr_3 = Ratio_1(dr_1) \tag{3.13}$$

Since equivalent radius r decreases continuously during grain refinement, r can be represented by

$$dr = -Ordt + IdW(t) \tag{3.14}$$

where O and I are constants.

For r_2 that decreases as a fraction of r during grain refinement, r_2 can be represented

$$dr_2 = Ratio_2(dr) \tag{3.15}$$

The models of strain for nanocrystalline material defined for the different approaches of measuring grain size evolution given in expressions (3.13)-(3.16) are

$$d\varepsilon_1 = d[dr_1 / r_1] = d\left(M\left(\frac{1}{r_{1c}}\right)\left(\frac{1}{r_1}\right) - \frac{1}{r_1^{\,2}}\right)dt + \frac{CDdW(t)}{r_1} - \frac{ZV_1\, r_1^{\,2} d(t)}{r_1} \tag{3.16}$$

$$d\varepsilon_3 = d[dr_3 / r_3] = d\left(\frac{Ratio_1 dr_1}{r_3}\right) \tag{3.17}$$

$$d\varepsilon_r = d[dr\ / r\ ] = d\left(\frac{-Ordt + IdW(t)}{r}\right) \tag{3.18}$$

$$d\varepsilon_2 = d[dr_2 / r_2] = d\left(\frac{Ratio_2 dr}{r_2}\right) \tag{3.19}$$

For other mechanical properties, the model of the Reversed Hall-Petch Relationship (RHPR) as modified by Zhao (Zhao et al., 2006:472) is given by

$$\sigma(r) = \sigma_0^{'} + A\left(r^{-\frac{1}{2}}\right) - B\left(r^{-1}\right) + C\left(r^{-\frac{3}{2}}\right) \tag{3.20}$$

3. A.2. 6 The Strain Rate Sensitivity (SRS) Modified Model

Another important mechanical property of superplastic material, is the high strain rate sensitivity of flow of stress (Vasin et al., 1997:1). The equation that relates material yield stress $(\sigma(r))$ and strain rate $(\dot{\varepsilon})$ is given in the form of a power law (Vasin et al., 1997:1) usually written as

$$\sigma(r) = K\dot{\varepsilon}^{m} \tag{3.21}$$

where m is the temperature dependent strain rate sensitivity (SRS) factor. By taking logarithms on both sides

of the equation the SRS is computed as

$$m = \frac{\log(\sigma(r))}{\log(\dot{\varepsilon})} \tag{3.22}$$

By employing the different models of strain (ε) for r, r_1, r_2 and r_3 during grain refinement, the strain rate $(\dot{\varepsilon})$ models for r, r_1, r_2 and r_3 during grain refinement are defined as or are modified to

$$d(\dot{\varepsilon}_1) = \frac{d\left[\frac{dr_1}{r_1}\right]}{dt} = \frac{d\left(M\left(\frac{1}{r_{1c}}\right)\left(\frac{1}{r_1}\right) - \frac{1}{r_1^{\,2}}\right)dt + \frac{CDdW(t)}{r_1} - \frac{ZV_1 r_1^{\,2} d(t)}{r_1}}{dt} \tag{3.23}$$

$$d(\dot{\varepsilon}_3) = \frac{d\left[\frac{dr_3}{r_3}\right]}{dt} = \frac{d\left(\frac{Ratio_1 dr_1}{r_3}\right)}{dt} \tag{3.24}$$

$$d(\dot{\varepsilon}_r) = \frac{d\left[\frac{dr}{r}\right]}{dt} = \frac{d\left(\frac{-Ordt + IdW(t)}{r}\right)}{dt} \tag{3.25}$$

$$d(\dot{\varepsilon}_2) = \frac{d\left[\frac{dr_2}{r_2}\right]}{dt} = \frac{d\left(\frac{Ratio_2 dr}{r_2}\right)}{dt} \tag{3.26}$$

3. A.2. 7 Deformation Activation Volume, Strain Rate Sensitivity and Processing Temperature of Grain Size Variants

The activation volume for plastic deformation which is directly related to the physical mechanism of deformation is given by (Gunderov et al., 2015:1).

$$V = \frac{\sqrt{3}K_B T}{m(\sigma(r))} \tag{3.27}$$

where K_B is the Boltzmann constant, *T is* temperature and *m* is the strain rate sensitivity. Equation (3.27) *revealed that the smaller the strain rate sensitivity the higher the activation volume*. The activation volume as given in equation (3.27) is determined by a relationship between the values K_B, *T*, m and $\sigma(r)$.

The strain rate sensitivity (m) varies with the increasing testing temperature on grain size variants. The dependence of the flow stress $\sigma(r)$ on the testing temperature T is ambiguous since melting temperature differs during grain refinement (Gunderov et al., 2015:1). All these activities account for the complexity of the dependence of the activation volume value on the testing temperature.

By employing the different modified models of strain (ε) for r, r_1, r_2 and r_3, and the modified models of strain rate $(\dot{\varepsilon})$ for r, r_1, r_2 and r_3, the activation volume of grain size variants is calculated.

Equations (3.4) to (3.27) are solved simultaneously using Engineering Equation Solver software (F-Chart Software, Madison, W153744, USA) and also employing the fact that, grain size distribution evolves as lognormal distribution (Tengen et al., 2009:461).

SECTION 3. B

After the derivation of the models, there was the need to perform experiments to validate the modified models. Two different experimental techniques were employed, which were ARB and ECAP.

3. B.1 Production of Nanomaterials by Accumulative Roll-Bonding (ARB)

3. B.2 Samples needed for Experimentations

Experimental Samples

- 6082T6 Aluminium

3. B.3 Apparatus for Experimental Set-up ARB

The Rolling mill apparatus/equipment

1) Two shafts which are to be place horizontally.
2) Two design support roll cage in which the two horizontal shafts rotate between
3) Two power generator and two chains to rotate the shaft by means of a mechanically automated operation
4) Support roll cage to ensure firm stability during deformation and bolts
5) Engineering glue (for stacking)
6) 4 Wire brushes
6) Cutting tool
7) Stop watch to measure the time of deformation
8) A pressure gauge to measure the applied force need to deform the sample

9) A temperature gauge to measure the room temperature during experiment

Figure 6: ARB Experimentation

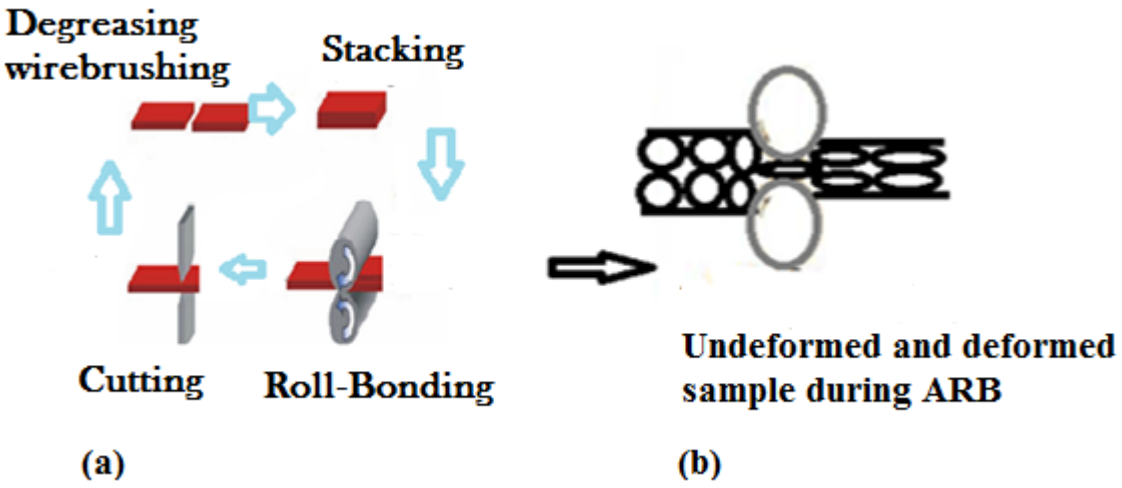

Figure 7: (a) Schematic of ARB process and (b) grain elongation

3.3. B. 4 ARB Experimentation

The experimental set up for ARB is shown in Fig.6. The ARB technology uses a conventional rolling facility. For this project two shafts were placed horizontally so that they were free to rotate by means of a mechanically automated operation. During experimentation the 6082T6 Aluminium was forced or fed through the rotating shafts. The rotating shafts gripped the 6082T6 Aluminium sample and forced the sample through the rollers in the first pass. The deformed 6082T6 Aluminium was cut into two pieces and stacked together. Before stacking, the entire surface of the strips were wire-brushed (i.e. using stainless steel brush) and degreased with tetrachloroethylene to achieve good bonding. The materials were joined together in the corners using aluminium wires and subsequently rolled. The whole sequence of "rolling, cutting, face-brushing, degreasing and stacking" was repeated again for several "passes" until nanomaterials with required characteristics were obtained. The samples with the deformed microstructures were examined using Transmission Electron Microscopy (TEM) to obtain lengths along the major axis r_3, semi major axis r_1 and semi minor axis r_2.

3.3.B. 5 ECAP Experimental Set-up

The apparatus needed for Equal-Channel Angular Pressing (ECAP).

1. ECAP die square work-piece
2. A hydraulic press or a plunger
3. An ingot

3.3. B.6 Experimental Procedure of Equal Channel Angular Pressing (ECAP)

The experiments were carried out as demonstrated by the routes in Figure 8 (c) and Figure 8 (d) using samples of 6082T6 Aluminium. It is recommended to design the ECAP die tunnels to intersect at an angle of 90^o but due to experimental difficulties the ECAP die tunnels were designed to intersect at angle φ approximately ($\varphi = 100^0$). During fabrication of nanomaterials, a hydraulic press was used to press the aluminium sample through the ECAP die as shown in Figure 8 (d). Since it was difficult to force the 6082T6 Aluminium sample through the ECAP die at the point where the two tunnels meet, the 6082T6 Aluminium samples were heat treated before each ECAP pass to enable the sample to pass through the ECAP die, as recommended by other researchers (Estrin et al., 2013:782). It should be marked that heating the 6082T6 Aluminium sample led to grain growth, and subjecting the material through the ECAP die led to grain refinement. Passes were repeated until the samples with the deformed microstructures were examined using TEM to obtain lengths along the major axis r_3, semi major axis r_1 and semi minor axis r_2.

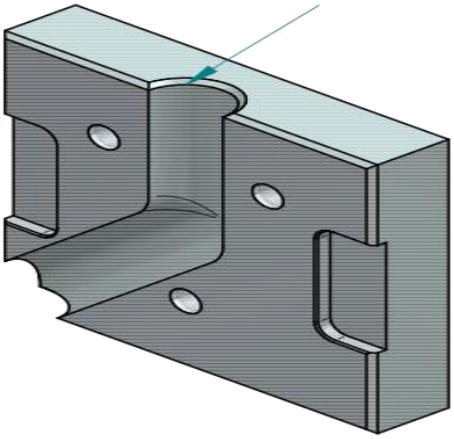

(a)

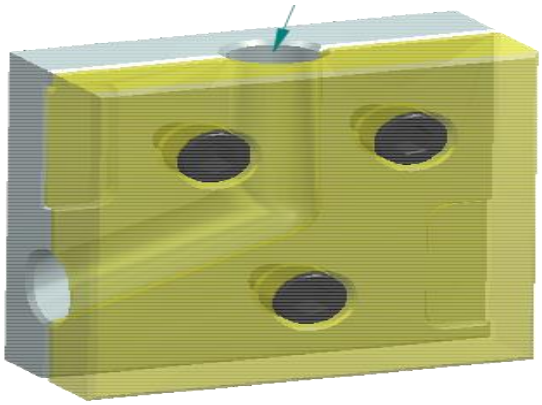

(b)

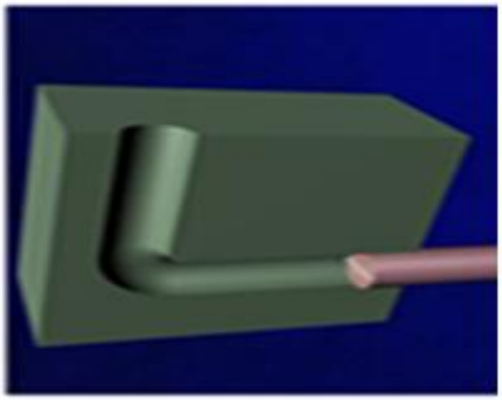

(c)

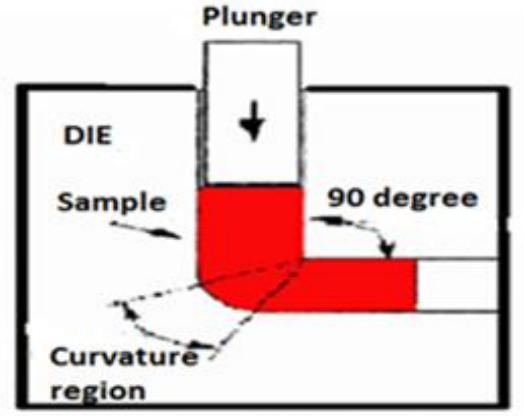

(d)

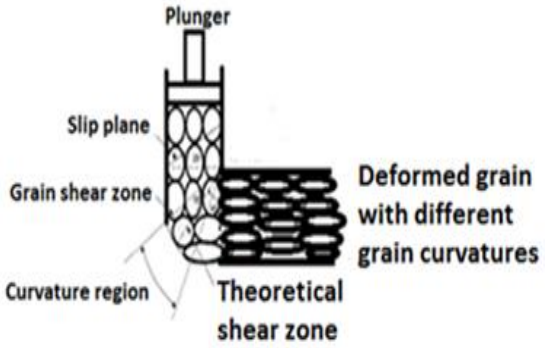

(e)

Figure 8: Experimental procedure for ECAP and schematic of ECAP processing routes, (b) schematic of material deformation and (c) schematic of grain refinement

SECTION 3. C

3. C.1 Sample Design for Mechanical Testing

In order to compare properties of materials deformed after different passes during grain refinement, it was necessary to design the samples for tensile testing as shown in figure 9.

Figure 9: Dog bone samples designed for mechanical testing.

In order to contain the little sample geometry, the dog bones were designed using the measurement of the gripping heads in which the dog bones could easily fit and screw into the universal testing machine as shown in figure 9. The actual set-up procedure for tensile test is given as follows. Before each testing period, the upper and lower grips are protected with the use of an alignment guide and alignment screws. The sample was clamped on both clamp members that were screwed to the lower and upper members of the universal testing machine.

3. C.1 Stress Testing (Mechanical Testing) and Data Capturing

The yield stress was measured during the deformation of nanostructured materials. The yield stress incurred by the dog bone samples were measured as shown in fig.10. The materials were subjected to longitudinal loading. Before experimentations by ARB the sample yield stress was measured and the sample for microscopic examination was removed for microscope study. After each processing route by ARB, a section of the material was cut for microscopic observation and tensile testing. The results of microscopic examination are shown in chapter four of this dissertation. The section of the materials taken for tensile testing was used to measure the yield stress of the materials in the different experimental cycles by ARB

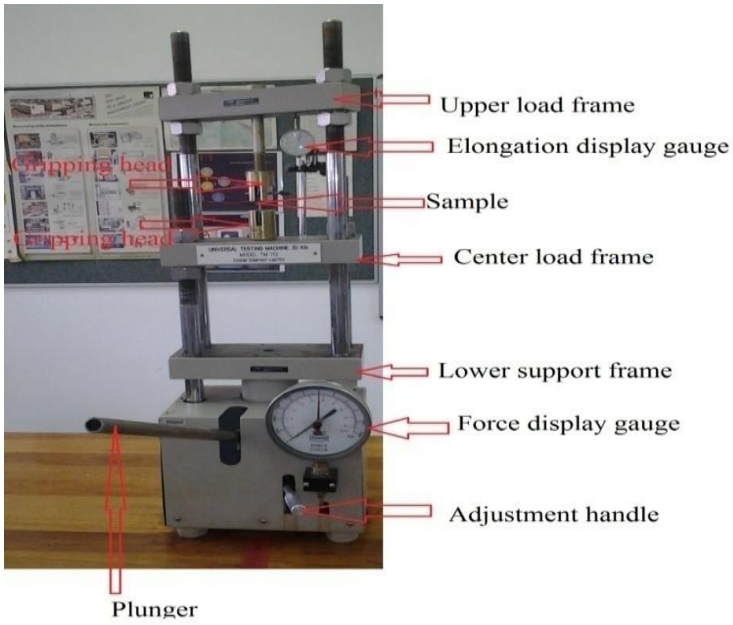

(a)

(b)

Figure 10: (a) Universal stress testing machine set-up and (b) Experimentation in progress

Figure 11: Dog bone samples after tensile test

3. C.2 Microscope Study

The initial sample with the deformed materials were examined using TEM. Standard TEM thin foils 3mm in diameter were prepared by electrolytic twin-jet polishing (at −30◦C, 30 V) in Struers Tenupol 2 filled with 6% solution of perchloric acid in methanol. The observations were carried out at 200 kV with JEOL JEM 2000FX microscope equipped with an X-ray energy dispersive spectrometer (XEDS)

LINK AN 10 000. Since theoretical models were already developed, it was necessary to measure the microstructures in the RD, ND and TD. The results are presented and discussed in chapter four.

CHAPTER FOUR
RESULTS AND DISCUSSION

The data from (nanocrystalline) aluminium sample (some of which are found in other papers (Tengen, 2008:40) are used to validate models, which are M_0'$=0.01nm^2s^{-1}$, $m=4$, $r_{c1}= 1.95r$, $CC=12$, $a=0.90$, $D=10^{-4}$, $h_0=0.25nm$, $T_m(\infty)=933.47K$, $CV_0=0.3$, $H_m(\infty)=10.71KJMol^{1}$, σ_0'$=16.7MPa$, $K_t=1.3$, $\sigma_0=15.40MPa$, $Kd=1301.77MPa\_nm^{1/2}$, $R=8.31JK^{-1}mol^{-1}$ and $T_r=300K$, $K_B=1.381023J/K$. Empirical data obtained for the different measures of size variants during experimentation is shown in table1.

Table 1: Empirical data obtained for the different measures of size variants during experimentations.

Cycles	Elongation[nm]	Yield stress [MPa]	Strain r	Strain rl	Strain r2	Strain r3	r [nm]	rl [nm]	r2 [nm]	r3 [nm]
Initial pass	7.856E-08	143	1	0.16	0.5	0.5	100	100	100	100
Passes	9.163E-08	220	2	0.5	0.8	0.9	97	95	60	98
Passes	4.502E-07	350	3	0.6	1	1	89	89	50	90
Passes	0.00013	150	3.3	0.7	1.3	1.6	60	40	30	60
Passes	0.0009	100	3.9	1	1.8	2	40	20	15	40

The additional data obtained for this work are $O=0.0035$, $I=1.1$, $r_0=100nm$, $Z=0.4$, $Ratio_1=0.81$, $Ratio_2=1.071$ and $\tau_1 = 0.000008$. The additional data were obtained through curve fitting of the empirical data from the different measures of the sizes from table: 1. The obtained results are presented in the plots and discussed below.

4.1Results of 2-D Grain: Time Evolution of Size [nm], Elongation [nm] and Size Ratio

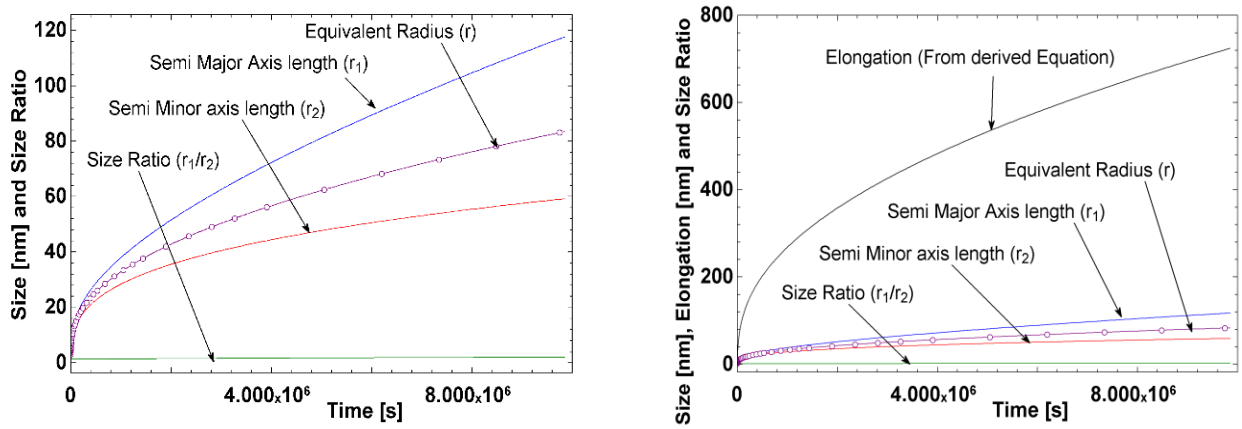

Figure 12: Time evolution of Size [nm], Elongation [nm] and Size Ratio

It has been revealed as shown in fig.12 (a & b) that the semi major axis length r_1 changes more rapidly with time than that of the semi minor axis length r_2 which is in line with grain elongation. As explained earlier, during refinement, as the grain size gets smaller, the semi minor axis length r_2 and the semi major axis length r_1 decrease. The size ratio (r_1/r_2) is the fraction of the semi major axis length r_1 and the semi minor axis length r_2. The size ratio (r_1/r_2) decreases at a very small rate during the deformation process. It is further observed that grain elongation varies more rapidly with time. Thus, all the measures of grain size changes in the same manner with time, as revealed in figure 12 (a & b).

4.2 Microstructures of Grain Observed by TEM and Properties (Yield stress and Elongation) along the TD and ND

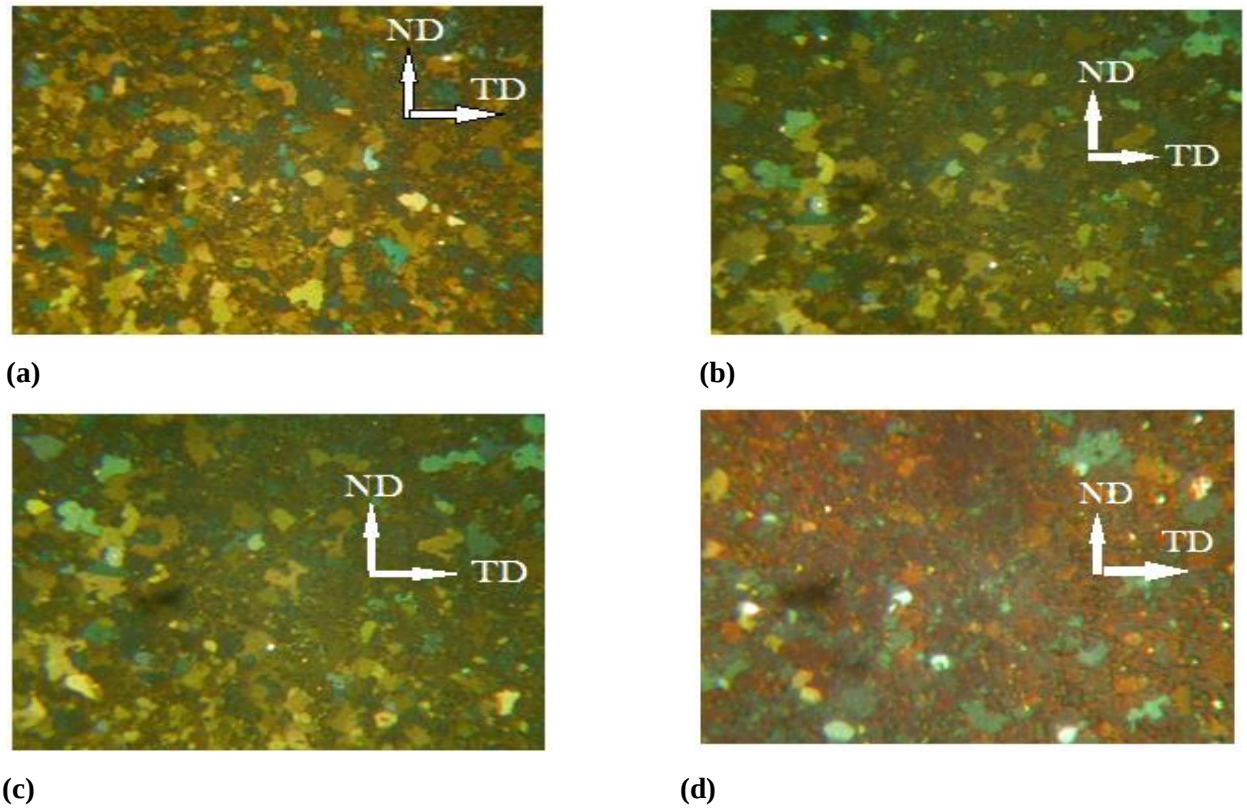

Figure13: Microstructures observed by TEM after different experimental cycles during grain refinement.

The observed microstructures of 6082T6 Aluminium samples are similar to those reported previously in literature, (Huang, Tsuji, Hansen & Minamino, 2003:*340*), (Kim, Lee & Shin, 2004:*449*) and (Kwan, Wang & Kang, 2008:*480*). The microstructures after a few experimental cycles are shown in Figure 13 (a & b) which consist of ultra-fine flow grains. After few experimental cycles the dislocations within these grains are low resulting to the occurrence of dynamic recovery process during grain refinement: a notion suggested by (Le, Tsuji & Kamikawa, 2006: 331). As more refinement takes place the low angle grains became large angle grains which enhanced material properties as shown in Figure 13 (d). The material has more enhanced properties

shown in figure 14 (a). The deformed materials experience more material flow along the TD (the semi major axis length r_1) with higher angle boundaries. This led to enhanced properties along the TD (the semi major axis length r_1) when compared to ND (semi minor axis length r_2) and the equivalent radius axis r. Figure 14 revealed the theoretical results from simulation of mechanical properties as functions of the different measures of size for 2-D grain during grain refinement.

4.3 Results of 2-D Grain: Plots of Yield Stress as a Function of Size [nm], Elongation [nm] and Size Ratio

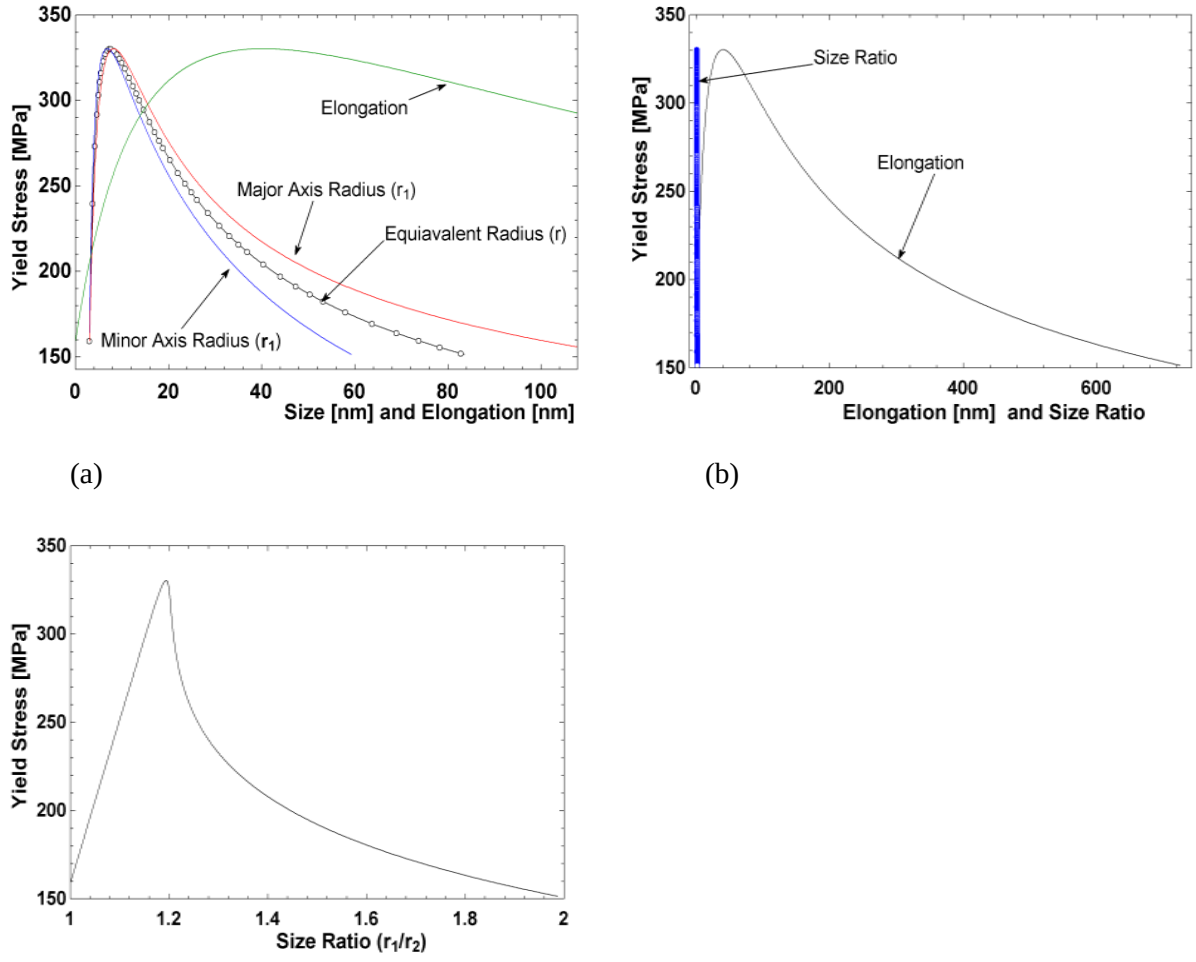

(a) (b)

(c)

Figure 14: Plots of Yield Stress as a function of (a) size (nm) and Elongation (nm) (b) Elongation (nm) and size ratio and (c) size ratio

These changes in the equivalent radius, semi major axis length and the semi minor axis length impact nanomaterials' mechanic properties such as yield stress. Observe from the plots of (Fig.14 (a-c)) that the evolution of yield stress as a function of grain size are of the nature of the Hall-Petch to Reverse-Hall-Petch Relationship: results similar to those observed by other researchers, (Tengen, 2008:96) (Whang, 2011:286) and (Whang, 2011:300). Observe further from (Fig.14 (a)) that obtaining the material yield stress as a function of

the different parameters, show that the material has the most enhanced properties when the grain gets more elongated. Obtaining the property with the size measured along the semi major axis length reveals a material with enhanced property following the one for elongation. The material with grain size measured along the semi minor length has least enhanced properties. While materials with grain size obtained as equivalent radius have property values that lie between those obtained with size measured along the semi minor axis length and the semi major axis length direction. Morris (Whang, 2011:53) observed that the strength of materials increased roughly twice after one cycle of ARB. Observe further that the relationship between the semi major axis length, equivalent axis radius and the semi minor axis length are obtained from expression (3-7), which is not an arithmetic average. Thus, one cannot claim that the evolution of the material property when related to equivalent axis radii can equally be obtained through the arithmetic mean of the properties obtained along semi major axis length and semi minor axis length.

The properties enhancement during deformation can be explained as follow: After several ARB cycles more grains boundaries are generated specifically lamellar boundaries with high angle grains having bigger misorientations (large misorientation-angle grain boundaries) that led to considerable high elongation as shown in Fig.13 (c-d) and 15 (a-d). This resulted in more elongated grains with higher angle boundaries as shown in Fig. 13 (d) and 15 (a-d). The trend revealed is similar to that reported by (Whang, 2011:45).

4.4 Grains Observed by TEM for Size Variants and Properties along the TD, ND and RD (3-D Observation)

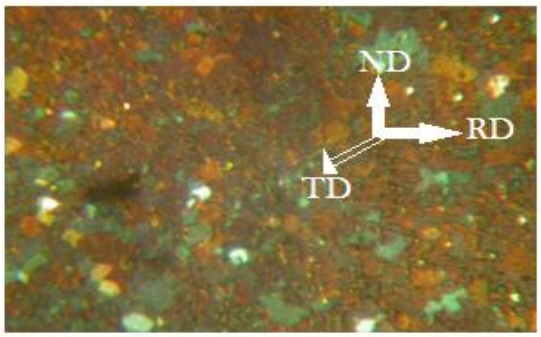

(a)

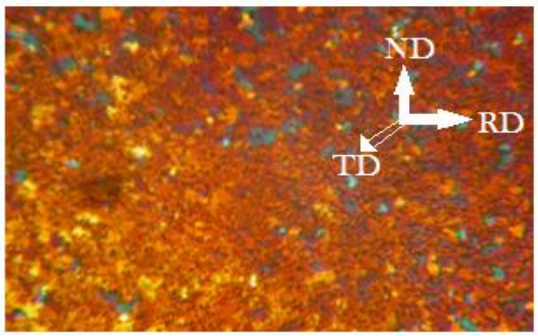

(b)

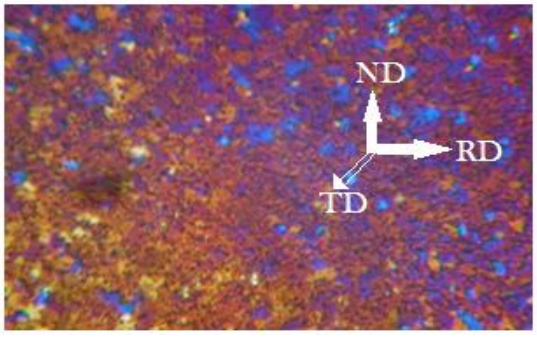

(c)

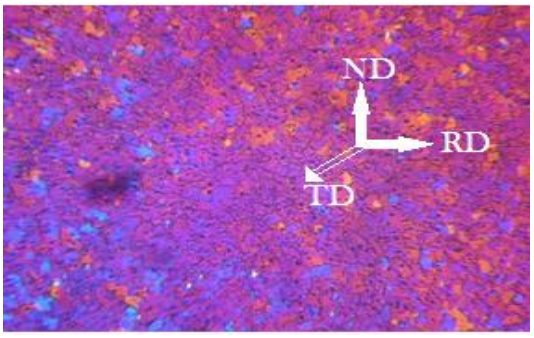

(d)

Figure.15: TEM observations after different experimental cycles during grain refinement.

Figure 15(a-d) revealed the microstructures of 6082T6 Aluminium samples after several experimental cycles. The TEM microstructures in Fig. 15 (a-d) showed that the grain size decreased as more refinement took place. Lamellar boundaries were observed in the microstructures along the RD (major axis r_3) direction as shown in Figure 15 (a-b). Dislocation boundaries were also generated in the RD (major axis r_3) direction. After several experimental cycles the microstructures showed a well-developed and homogenous lamellar structure as shown in Figure 15 (c-d) respectively. The boundaries along the RD (major axis r_3) and direction TD (semi major axis r_1) direction are higher than the boundaries in the ND (semi minor axis length r_2). This resulted in higher material properties along the RD (major axis length r_3) and TD (semi major axis length r_1) when compared to the ND (semi minor axis length r_2). The grain boundaries decrease with increasing strain during grain refinement. The results in Figure 16 revealed the theoretical results from simulation of the different measures of size for 3-D grains during grain refinement.

4.5 Results of 3-D Grain: Plots of Size [nm] as a Function of Time [S] and Elongation [nm] as a Function of Time [s] and Size [nm].

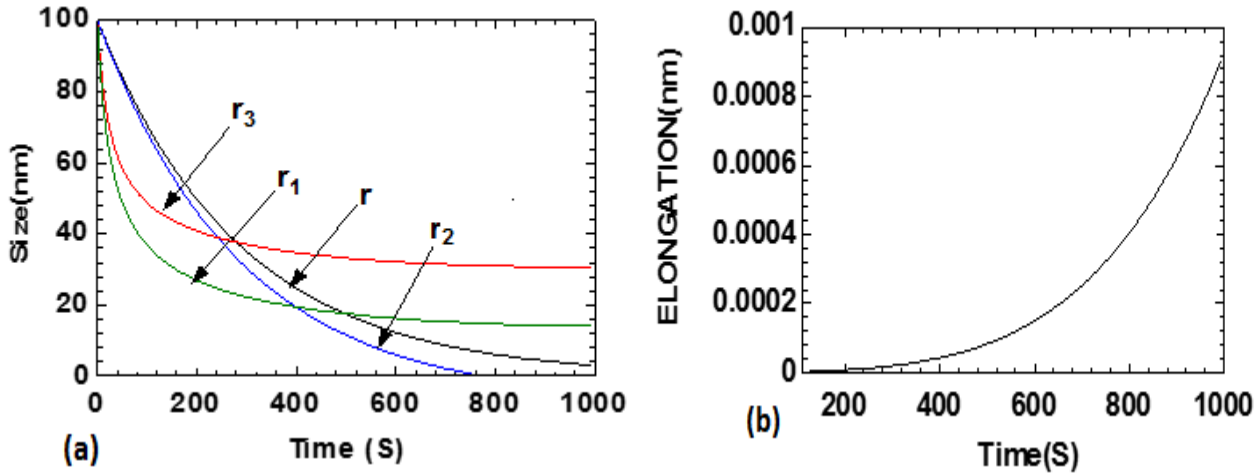

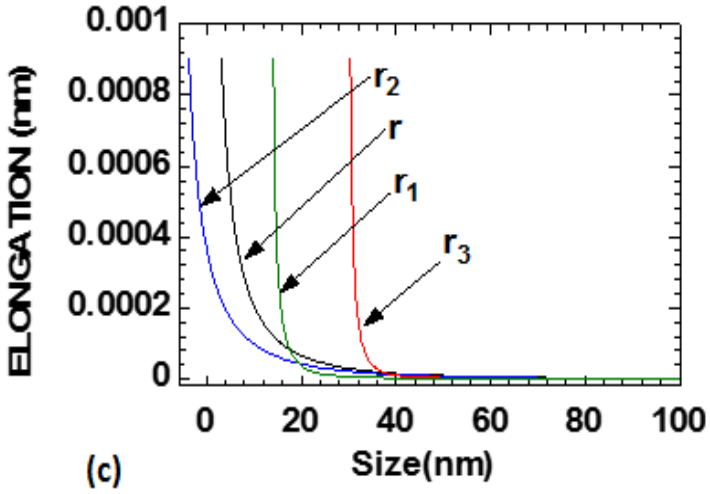

Figure 16: (a) Time evolution of size (nm), (b) time evolution of elongation (nm) and (c) evolution of elongation as a function of size (nm).

The Plots of figure 16 (a) were obtained from empirical data of table 1. It should be observed from Fig.16 (a) that, r_2 decreases to a lower value when compared to r throughout the deformation process, and similarly, r_1 decreases to a lower value when compared with r_3 throughout the deformation range. It was also observed and revealed that both r_1 and r_3 initially started with breakage and as such smaller grain sizes, which then lengthened and became larger than those sizes of r and r_2. The increase in grain elongation with time as shown in Fig.16 (b) or with decreasing grain size as shown in Fig.16 (c) can be explained by the fact that during grain refinement, new high angle grain boundaries are generated. It should be observed further from Fig. 16 (c) that the grain elongations were observed to evolve as the same small value for larger grains when the size was measured along all the different directions, but the grains became highly elongated, with varying values, as the grain sizes were approaching zero. It should further be observed that the grain size at which elongation became so large was not unique and depended on the approach of measuring the grain size. In the directions where the grains lengthen followed by breakage, it was revealed that the elongation became so large at smaller grain size values that was larger when compared with the size measured along the directions where there was a continuous decrease in grain size.

4.6 Grains Observed by TEM for Size Variants and Properties (Strain) along the TD, ND and RD (3-D Observation)

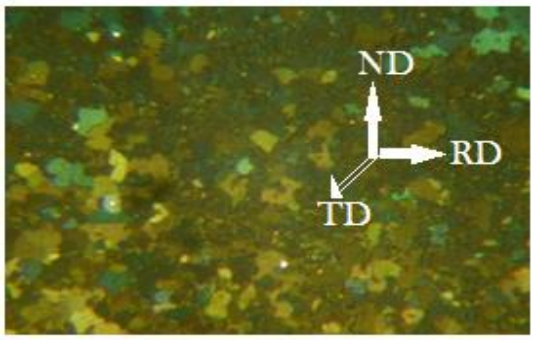

(a)

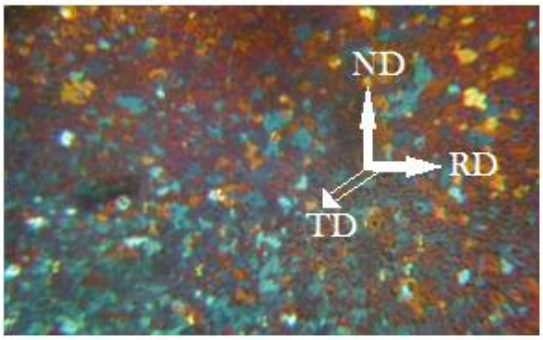

(b)

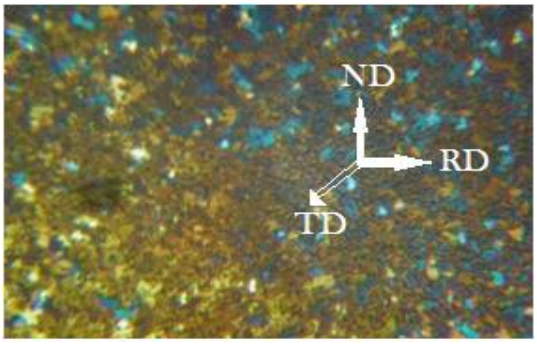

(c)

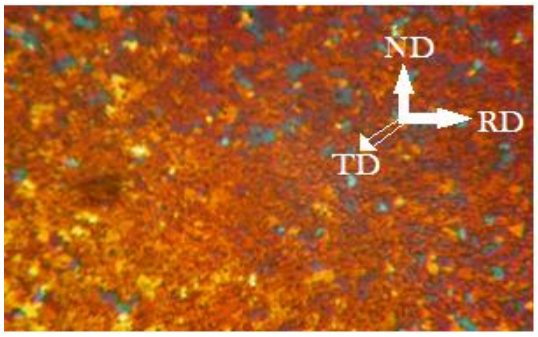

(d)

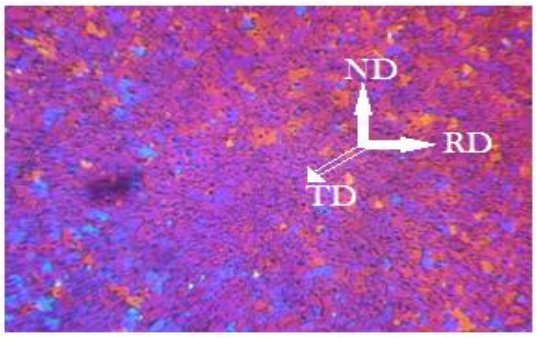

(e)

Figure17: TEM observations after different experimental cycles during grain refinement.

During investigation of the strains on the microstructures, it was observed after a small number of experimental cycles that there is a mixture of grains that have not deformed and grains that suffer a reduction in thickness and an elongated morphology oriented in the RD as shown in Figure 17 (a). After several experimental cycles the orientation of the grains can be seen as shown in Figure 17 (b). They are two different types of grains coexisting in Figure 17 (b), the equiaxial and morphologically elongated grains. After further experimental cycles severe reduction of thickness of grain size is shown in Figure 17 (c). The grain boundaries become less visible since the grains are thinner and elongated in the rolling direction as shown in Figure 17 (c). As the number of experimental cycles increase the microstructures show a more uniform structure as shown in Figure

17 (d). The material strain is very high due to a large number of experimental cycles of grain refinement. The dislocations density is high due to the high deformation suffered by the material during continuous straining of the material.

As the number of experimental cycles increase the microstructure obtained is shown in Figure 17 (e), from where it is possible to observe recrystallization. The material is continuously recrystallizing as observed in Figure 17 (e). This is characterized by grain subdivision of ultra-fine grains which are recovered to form new ultra-fine grains with migration of grain boundaries. The material suffers a breakage of the laminar structure due to surface stress and strain that is generated during grain refinement on the TD, ND and RD. The critical condition of grain breakage occurs when the size of the grain is very small during grain refinement. When the size of the grain is stable, the movement of free dislocations is shorter and the formation of dislocation in the grain is limited. The motion of dislocations is characterised by easy slip without any blockage inside the grain and this creates sub-cells that result in dynamic recovery. As more grain refinement takes place grain growth occurs due to adiabatic warming.

4.7 Results of 3-D Grain: Plots of Strain as a Function of Time [S] and Size [nm].

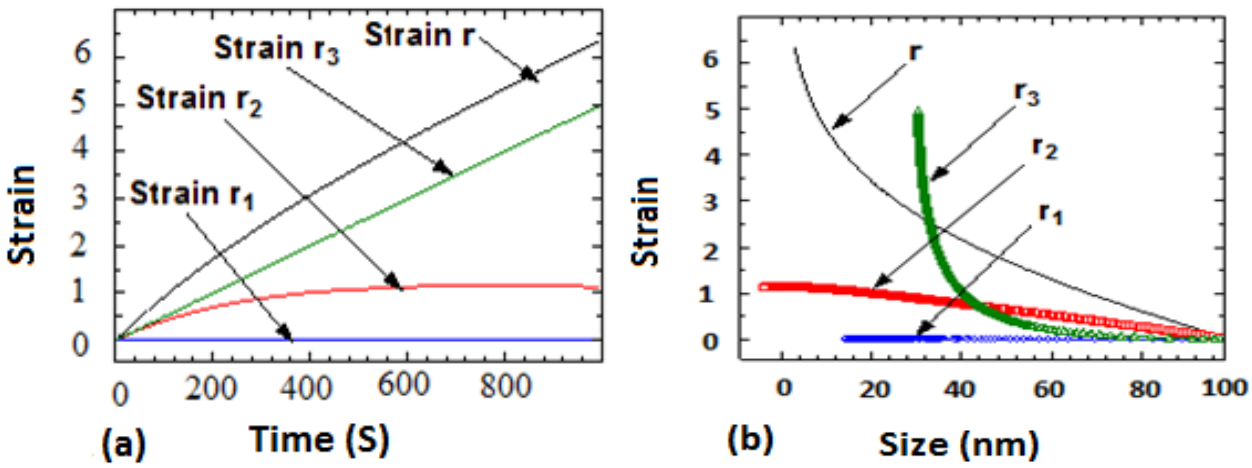

Figure 18: (a) Time evolution of strain and (b) strain evolution of size (nm)

Figure 18 proves that the grain strain values could not be directly inferred from the plots of the evolutions of different measures of grain size given in Figure 18 (a). While the strain values were revealed to all increase with time, the use of equivalent radii gives larger strains, followed by strains measured along the major axis length and least by semi major axis length. While comparing the grain strain variations with different approaches of measurement of the grain size (see Fig.18 (b)), the strains evolved are initially at lower values for sizes measured along the directions where the grains lengthened followed by breakage, and this relationship changed at the point where the grain elongation exploded or at smaller grain sizes i.e. the strains also became larger. It can be concluded that different approaches of measuring grain size, reveal different values of strain

that cannot be directly obtained from plots of the evolution of grain sizes. Observed from Fig. 18 (a-b) it can be seen that at larger grain size (100-80nm) the strain experienced by the grain size variants is less than 0.5. As more grain refinement takes place the grain size became very small resulting in higher strain values of the grain size variants.

4.8 Results of 3-D Grain: Plots of Yield Stress [MPa] as a Function of Time [S], Size [nm], Elongation [nm], Strain and Strain rates [1/S].

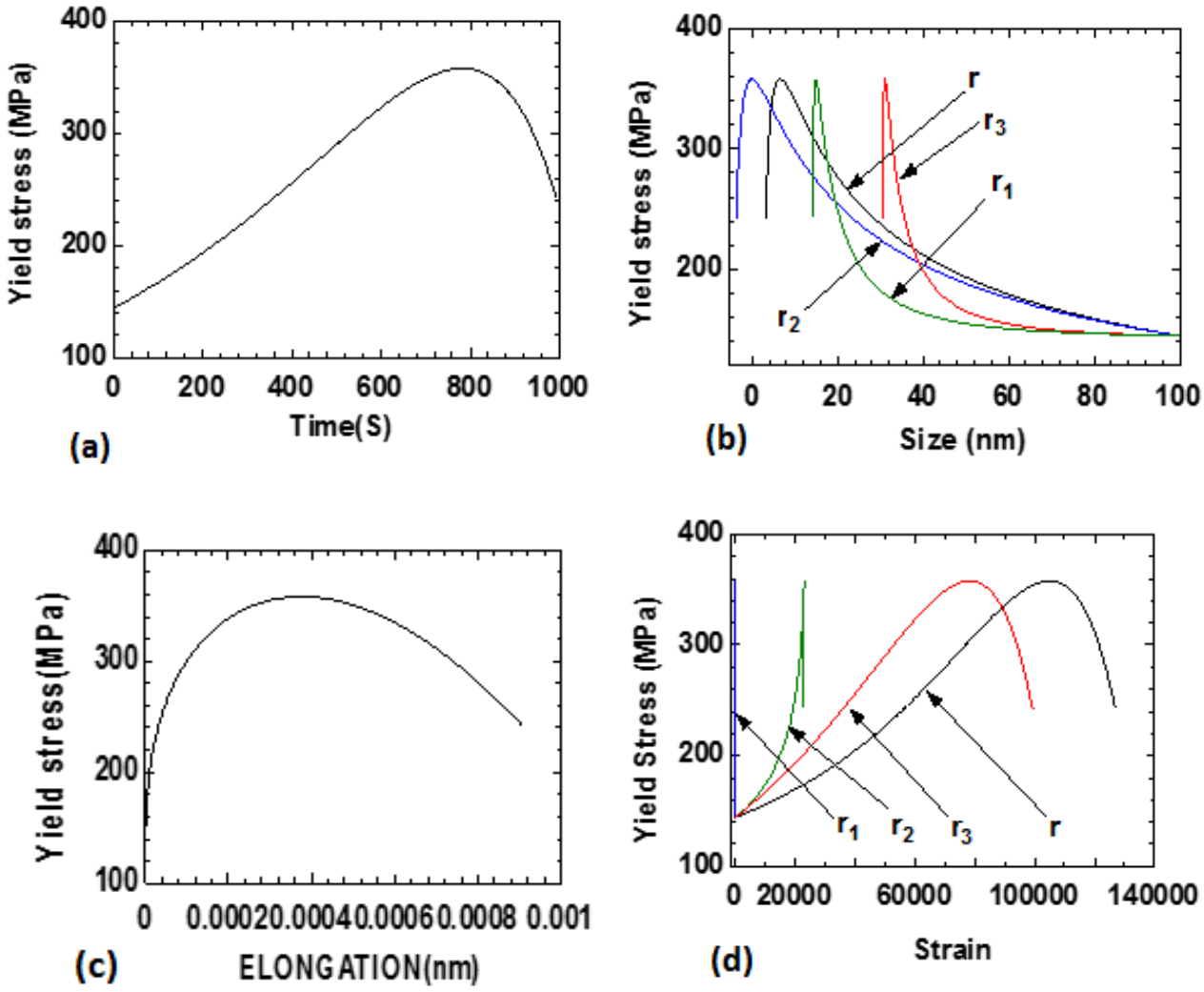

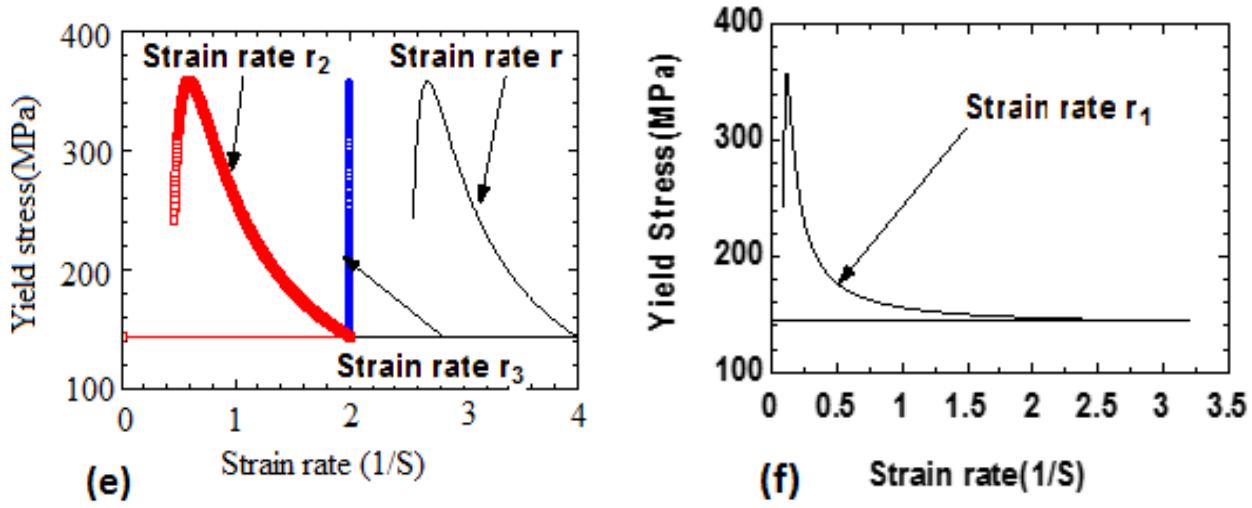

Figure 19: Plots of yield stress as a function of (a) time, (b) size (nm), (c) elongation (nm), (d) strain, and (e-f) strain rate

From Fig.19 (a-f) it is observed that yield stress evolved as predicted by Hall-Petch to Reversed Hall-Petch Relationship (HPR-RHPR) when measured as functions of time, different approaches of measuring grain size, elongation, strain and strain rate. The yield stress generally increased with decreasing grain size since this was accompanied by dislocation motion from grain interiors to grain boundaries and subsequent dislocation pile-ups at the grain boundaries. It was observed that in the directions where the grain sizes increased and subsequently decreased due to grain breakage (i.e. r_1 and r_3), there were more material flow in those directions, accompanied by more dislocation motions, dislocation pile-ups, and hence larger grain boundary curvatures in those direction.

The yield stress when measured as a function of grain size and strain with grain size measured along the r_1 and r_3 directions showing more rapid enhanced properties (see Fig.19 (b) & (d)). Since elongation can be termed lengthening, it can be concluded that materials with elongated grains have more enhanced properties which rapidly drop with continuous lengthening of the grains. The reason for the subsequent decrease in yield stress with further increase in elongation was due to the fact that there came a point where the elongation became extremely large with very small changes in grain size leading to low plastic deformation and low materials hardness. Extreme plastic straining led to distorted structures where the grain boundaries and grain curvatures were in "non- equilibrium" states. Furthermore, it has been revealed as shown in Fig.19 (b) that different critical grain sizes exist for r_1, r_2, r_3 and r, but at the same yield stress value.

The different strain rates observed in Fig.19 (e) and (f) show a general trend. It should be observed that in order to increase the material yield stress, the rate of straining of the material had to be reduced which was in line with the observations made by other researchers (Barnett, Estrin, Hodgson & Sabirove, 2009:181). The reduction in strain rate was to allow the material to relax and accommodate more plastic strain. Furthermore,

it was observed that indefinite reduction in strain rate did not lead to more property enhancement since it was becoming difficult for the material to deform.

4.9 Results of 3-D Grain: Plots of Strain rate [1/S] as a Function of Size [nm]

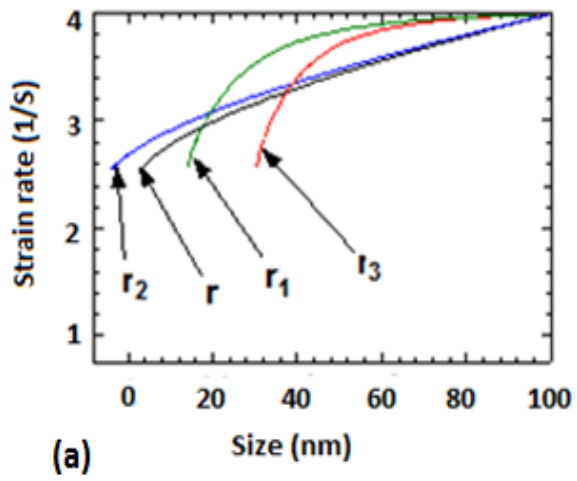

Figure 20: Plots of strain rate as a function of size (nm)

4.10 Results of 3-D Grain: Plots of Yield Stress [MPa] as a Function of Strain Rate [1/S) and Material SRS Calculated at the slops of Grain Size Variants at Different Temperatures.

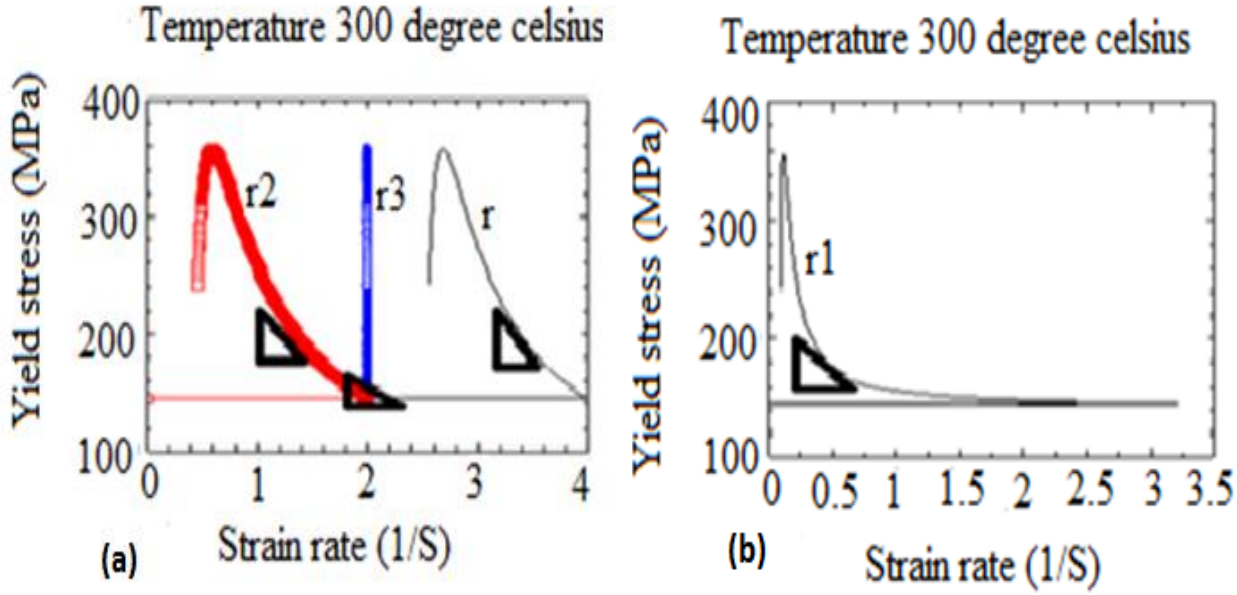

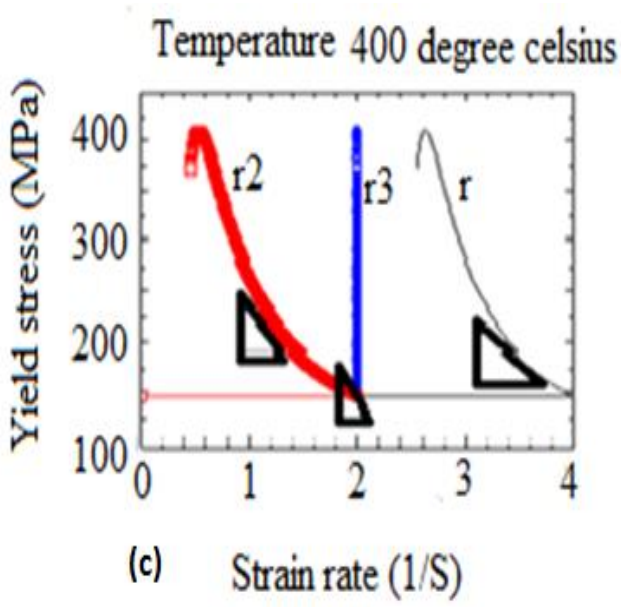
Temperature 400 degree celsius
Yield stress (MPa)
400
300
200
100
0
1
2
3
4
r2
r3
r
(c)
Strain rate (1/S)

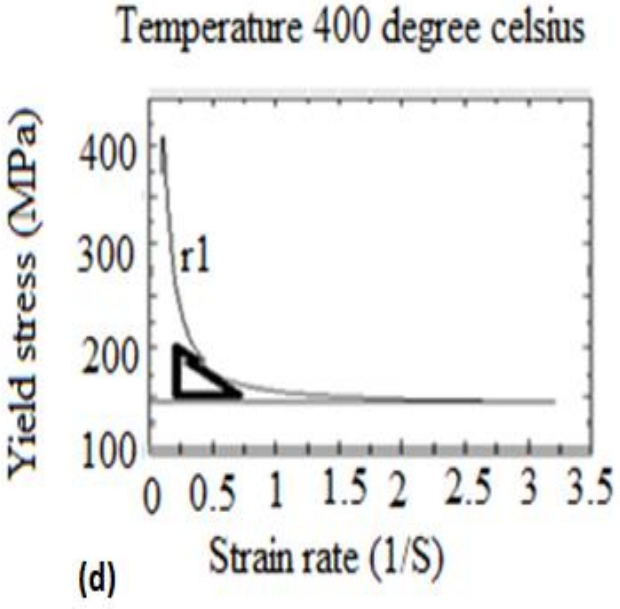
Temperature 400 degree celsius
Yield stress (MPa)
400
300
200
100
0
0.5
1
1.5
2
2.5
3
3.5
r1
(d)
Strain rate (1/S)

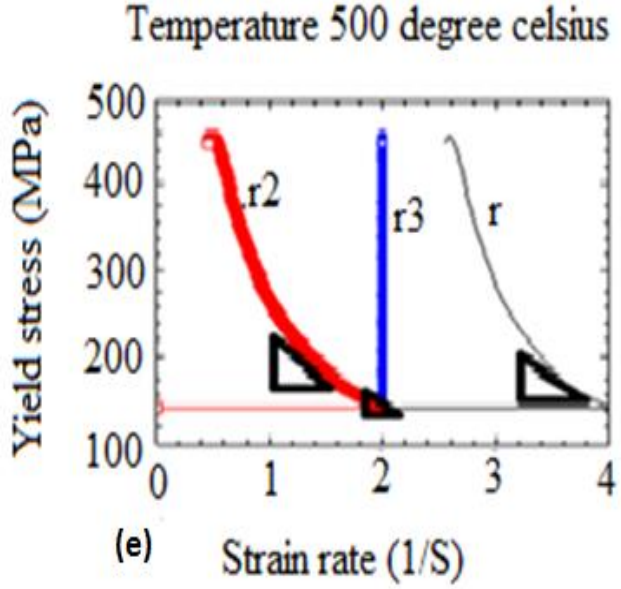
Temperature 500 degree celsius
Yield stress (MPa)
500
400
300
200
100
0
1
2
3
4
r2
r3
r
(e)
Strain rate (1/S)

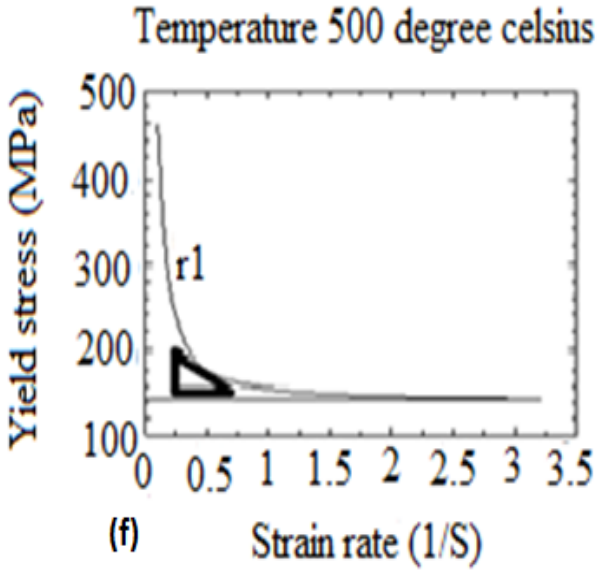
Temperature 500 degree celsius
Yield stress (MPa)
500
400
300
200
100
0
0.5
1
1.5
2
2.5
3
3.5
r1
(f)
Strain rate (1/S)

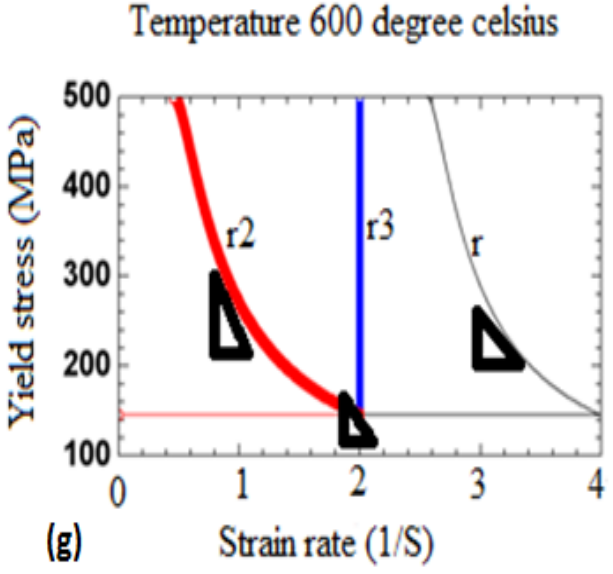
Temperature 600 degree celsius
Yield stress (MPa)
500
400
300
200
100
0
1
2
3
4
r2
r3
r
(g)
Strain rate (1/S)

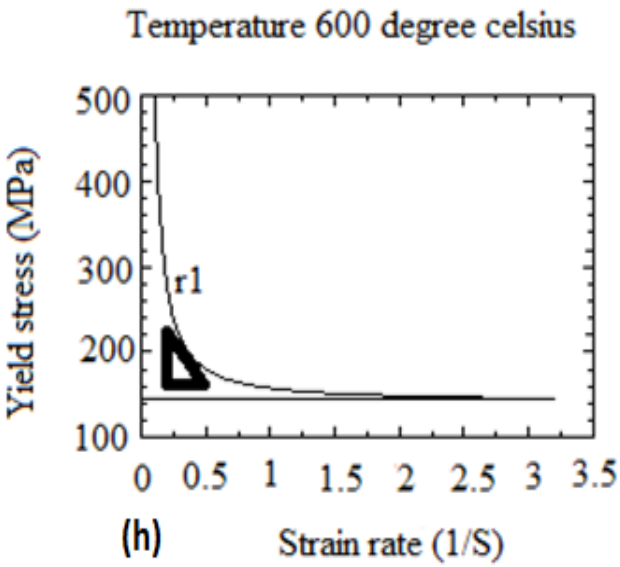
Temperature 600 degree celsius
Yield stress (MPa)
500
400
300
200
100
0
0.5
1
1.5
2
2.5
3
3.5
r1
(h)
Strain rate (1/S)

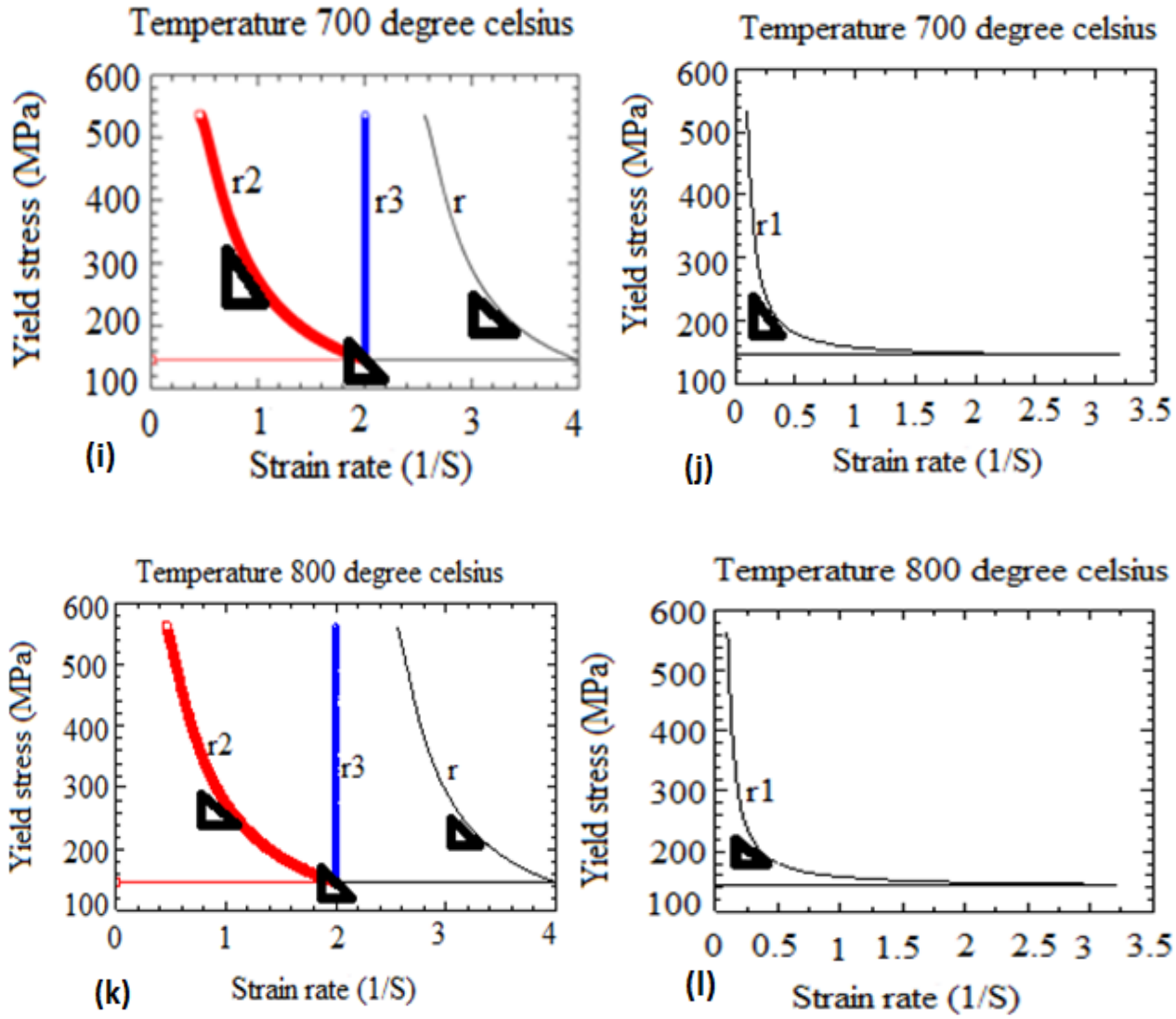

Figure 21: Plots of yield stress and strain rates at different temperatures; and SRS calculated at the slops of the grain size variants.

The SRS values for the grain size variants were calculated from the slopes of the plots at different temperatures of $d(\log(\sigma(r)))$ against $d(\log(\dot{\varepsilon}))$. These values are presented in Table 2.

Temperature (°C)	(SRS) r_1	(SRS) r_2	(SRS) r_3	(SRS) r
300	-5.66	-5.67	-5.91	-8.65
400	-5.74	-6.33	-4.54	-12.12
500	-6.13	-19.07	-2.83	-11.61
600	-3.40	-5.03	-4.64	-4.78
700	-4.47	-5.03	-4.47	-18.35
800	-4.03	-4.03	-4.67	-4.67

Table 2: The results of SRS measurement at six temperatures on grain size variants

4.11 Grains Observed by TEM for Size Variants and Properties (SRS and Deformation Activation Volume) along the TD, ND and RD (3-D Observation)

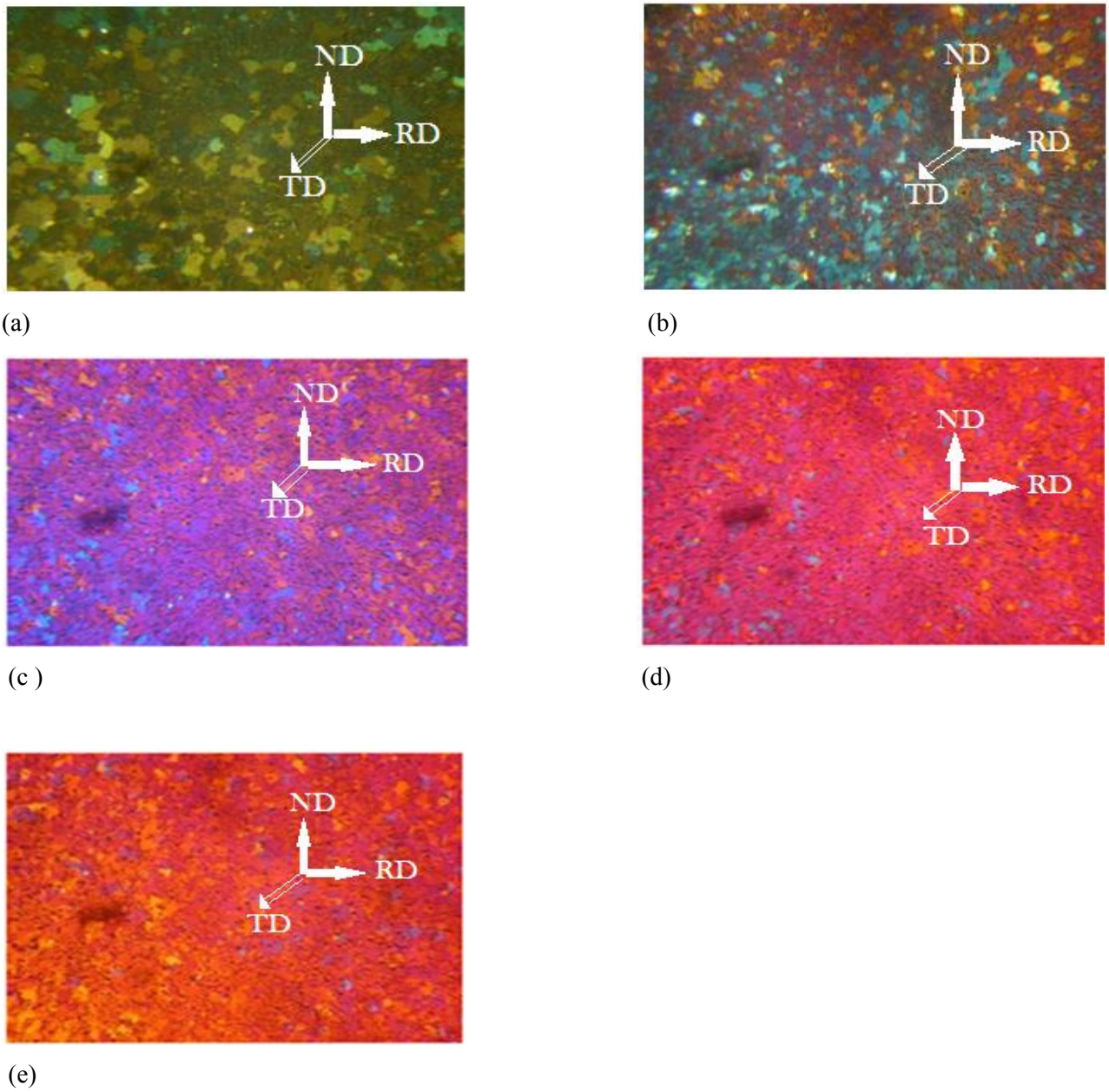

Figure 22: TEM observations after different experimental cycles during grain refinement.

Figure 22 (a-e) shows the microstructure of the material as the number of experimental cycles increased. It is observed that the grains get finer as the number of experimental cycles increased as shown in Figure 22 (a-e). Figure 22 (d-e) indicates the presence of tiny grains which are randomly oriented after several experimental cycles. Grain size affects the activation volume of the flow of stress during grain refinement. Dislocation gliding and the multiplication of dislocations are the dominant mechanisms in plastic deformation. When the material's grains were refined to small sizes, the dislocation glide mechanism was suppressed and the GBs

became dominant which led to an increase in SRS. As more experimental cycles took place with a further decrease of grain size, nucleation and movement of lattice dislocations were suppressed severely by the ultrafine grains in Figure 22 (d-e). It has been suggested that GB diffusion could dominate the rate sensitivity for the materials within the nano-scale range of grain sizes (Van Swygenhoven, Spaczer & Caro, 1999:1). Since different grain sizes existed with different grain curvatures along the TD, ND and RD, the higher amount of high angle grain curvatures was the main reason for the enhanced SRS and the lower amount of low angle grain curvatures was the main reason for a lower SRS for grain size variants during grain refinement.

After a small number of experimental cycles as shown in Figure 22 (a-b) lamellar boundaries were observed in the microstructures along the RD (major axis length r_3). Dislocation boundaries are also generated in the RD (major axis length r_3). After more experimental cycles the microstructures showed a well-developed and homogenous lamellar structure as shown in Figure 22 (c-d and e) respectively. The number of boundaries along the RD (major axis length r_3) and TD (semi major axis length r_1) were higher than the number of boundaries in the ND (semi minor axis length r_2) direction. This resulted to a higher SRS along the RD (major axis length r_3) and TD (semi major axis length r_1) directions when compared to the ND (semi minor axis length r_2) direction. Since the grain curvatures varied continuously during grain refinement, the SRS continuously increased and decreased during grain refinement due to high and low angle grain curvatures of the grain size variants.

This research suggests that as the grain size is reduced as shown in Figure 22 (a-e) not only does the yield stress (strength) increase but the SRS also increases. However, during grain refinement from micrometre to nanometre scale the activation volume decreased with the material grain size variants. The increase of the SRS on grain size variants is directly related to a change in the rate controlling mechanism for plastic deformation. It is seen from equation (3-27) that $m = \frac{1}{V}$ i.e. where m is inversely proportional to the activation energy. An increase in SRS led to a decrease in activation volume whereas an increase in activation volume led to a decrease in SRS. The results in Figure 23 to Figure 26 reveal the theoretical results from simulation of SRS and deformation activation volume for the different measures of size for 3-D grain during grain refinement.

4.12 Results of 3-D Grain: Plots of SRS as Functions of Temperature [^{o}C]

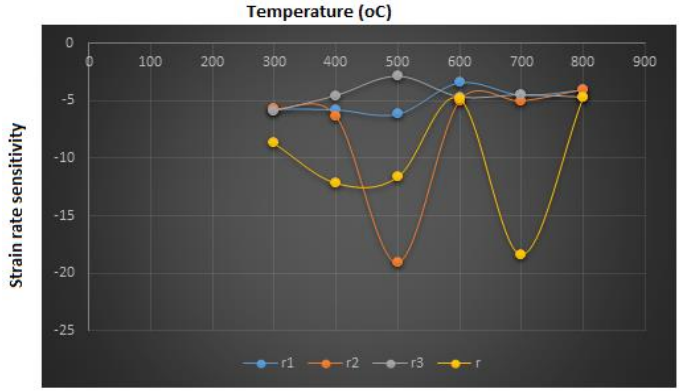

Figure.23: Variation of (SRS) with Temperature at six temperatures within the negative SRS range for grain size variants

4.13 The Sensitivity of Nanomaterials

The variations of SRS with temperature are shown in Figure 23 for six different temperatures. It is observed that at a temperature range from room-temperature up to 400°C, no pronounced SRS is found for r_1. By increasing the testing temperature further (above 400°C), the SRS was also increased and decreased for the grain size variants. The different results of SRS for the different grain size variants were due to different grain curvatures during grain refinement. The higher number of high angle grain curvatures was the main reason for the enhanced SRS and the lower number of low angle grain curvatures was the main reason for a lower SRS for grain size variants. The results obtained indicated a change in the deformation mechanism of the ultra-fine grain regime due to different grain curvatures during grain refinements. The thermal activated recovery processes taking place at the grain curvatures, were the dominating deformation mechanisms.

Studying curvature on SRS, it was observed from Figure 23 that at a temperature of 400°C different SRS were revealed. From the different SRS revealed at a temperature of 400°C the material SRS was high for lengths measured along r_3 due to higher grain curvature of r_3 when compared with the curvatures of r_2, r_1 and r. At a temperature of 500°C the SRS increased along r_3 and decreased along r_1, r and r_2 due to higher grain curvature of r_3 when compared with the curvatures of r_1, r and r_2. The SRS decreased more along r_2 when compared to r_1 while r and r_3 increased at a temperature of 400°C to 500°C since the grain curvature of r_2 was lower than the curvature of r_1, r and r_3. *The variation of SRS with temperature in grain size variants suggests that the SRS for 6082T6 aluminium at the low and the high temperature ends are different*. This suggests that different dynamic strain aging (DSA) mechanisms dominate the behaviour of r_1, r_2, r_3 and r at different temperature ranges, since at extremely low temperatures the SRS was small and at high temperatures the SRS increased and resulted of material hardening. The high temperature behaviour did not appear to be due to structural changes such as precipitation, which could change the nature of the rate controlling obstacles to dislocation motion. From this study it has been revealed that nanomaterials are very sensitive to temperature during manufacturing.

4.14 Results of 3-D Grain: Plots of SRS as Functions of Size [nm].

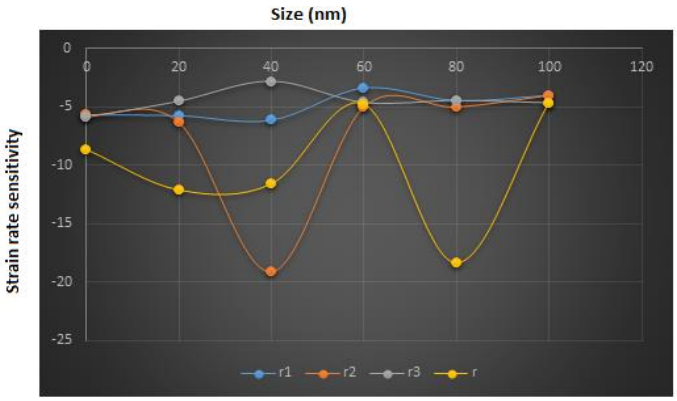

Fig. 24: (a) Variations of the strain rate sensitivity (m) with size (nm) at six temperatures within the negative SRS range

The primary reasons for increases and decreases in SRS were due to different grain curvatures, grain boundary diffusion, grain boundary sliding mediated by dislocation activity and controlled plasticity on the grain size variants during grain refinement. It is observed from Figure 24 that the SRS varied in different ways with grain size variants due to different grain curvatures. It is observed from Figure 24 that at a grain size of 20nm different SRS values were revealed for the grain size variants. From the different SRS values revealed at a grain size of 20nm the material SRS was high for lengths measured along r_3 and low for lengths measured along r, r_1 and r_2 since the grain curvature of r_3 was higher than the curvatures of r, r_1 and r_2. It was observed, at a grain size of 40nm, that SRS increased when measured along r, r_1, r_2 and decreased along r_3 due to higher grain curvatures of r, r_1, r_2 and lower grain curvature of r_3. It was also observed at a grain size of 60nm to 80nm that the SRS increased along r_3, r_1, r_2 and decreased along r. It was further observed at a grain size of 100nm that the SRS increased more along r when compared to r_1, r_2 and r_3 due to higher grain curvatures of r.

The results in Fig. 24 show a clearly that the SRS continuously increased and decreased at different temperatures for the grain size variants. The increase in SRS was directly related to a change in the rate controlling mechanism for plastic deformation. There have been reports of both increased and decreased SRS with decreasing grain size in metals (Meyer et al. 2006:456), similar to the results obtained in this research.

4.15 Material Deformation Activation Volume, Strain rate sensitivities and Processing Temperatures on Grain Size Variants

T (oC)	V(r1)	V(r2)	V(r3)	V(r)	m(r1)	m(r2)	m(r3)	m(r)
300	-45642.4	-45562	-43712	-29865.5	-5.66	-5.67	-5.91	-8.65
400	-70009.8	-63484.4	-88514.6	-33156.5	-5.74	-6.33	-4.54	-12.12
500	-89748.9	-28849.5	-112238.6	-27358.8	-6.13	-19.07	-2.83	-11.61
600	-219501.4	-148371	-160842	-156131	-3.40	-5.03	-4.64	-4.78
700	-202278	-179757	-202278	-49274	-4.47	-5.03	-4.47	-18.35
800	-275407	-275407	-237664	-237664	-4.03	-4.03	-4.67	-4.67

Table 3: The results of activation volume and SRS measurement at six temperatures on grain size variants.

4.16 Results of 3-D Grain: Plots of Activation Volume as a Function of Temperature [ºC]

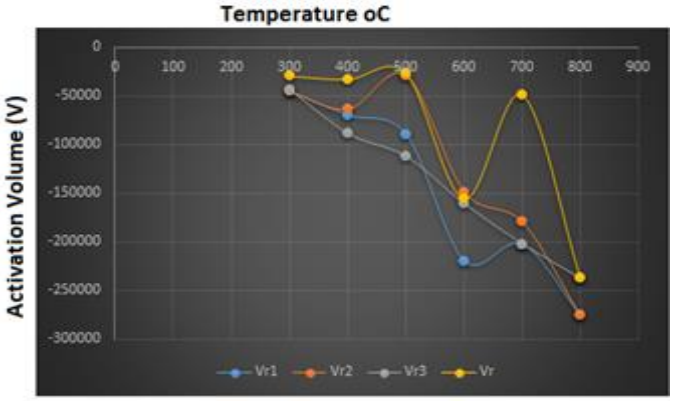

Figure 25: Variation of activation volume (V) with Temperature at six temperatures within the negative activation volume range for temperature

4.17 The Activation Volume and Processing Temperatures on Grain Size Variants

The variation of activation volume with temperature is shown in Figure 25 for six different temperatures. It was observed that at a temperature range from room temperature up to 400ºC, no pronounced activation volume was found for r whereas the activation volume decreased along r_2, r_1 and r_3. By increasing the testing temperature further, the activation volume also increased and decreased for the grain size variants. The different results of activation volume on grain size variants were due to different grain curvatures during grain refinement. The higher number of high angle grain curvatures was the main reason for the lower activation volume and the lower number of low angle grain curvatures was the main reason for a high activation volume on grain size variants. The above results indicate a change in the activation volume during grain refinement for the grain size variants due to different grain curvatures. It is, however, noted that the activation volume characterizes the stress sensitivity of dislocation velocity which is related with the dislocation process of

different grain curvatures of the grain size variants. It is also based on the thermally activated plastic deformation process of the grain curvature of the grain size variants. The dislocation velocity depended on the activation energy and also the shear stress acting on the dislocation that was characterized by different grain curvatures on the grain size variants during grain refinement.

Looking at the effect of different grain curvatures, grain boundary diffusion, grain boundary sliding mediated by dislocation activity on activation volume for the grain size variants during grain refinement, it is observed from Fig. 25 that, at a temperature of 400^{o}C, different activation volumes were revealed for the grain size variants. From the different activation volumes revealed at a temperature of 400^{o}C the material activation volume was lower for lengths measured along r_3 since the grain curvature for r_3 is higher when compared with the curvatures of r_2 and r_1. When the testing temperature increased from 400^{o}C to 500^{o}C the activation volume was still lower along r_3 and r_1, and increased along r_2 and r since the grain curvatures of r_3 and r_1 were higher when compared with the curvatures of r_2 and r. The increase in activation volume with increase in testing temperature could also be rationalized based on the fact that during grain refinement of 6082T6 aluminium there was a martensitic (crystal structure) state. And the grain size variants were characterized by lower grain curvatures. It has been revealed that, the SRS tends to increase with temperature on grain size variants due to higher grain curvatures, whereas the effect of temperature on activation volume decreased with higher grain curvature.

4.18 Results of 3-D Grain: Plots of Activation Volume as a Function of Grain Size [nm]

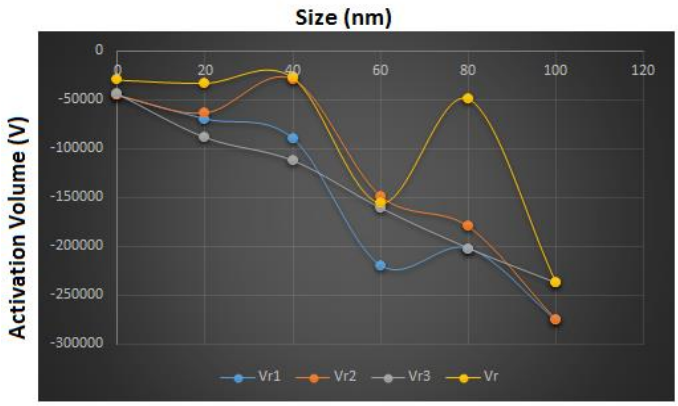

Figure.26: Variation of activation volume (V) with Size (nm) at six temperatures within the negative activation volume range for grain size variants.

The main reasons for the increase and decrease in activation volume was due to different grain curvatures on the grain size variants as already explained. It is observed from Figure 26 that the activation volumes varied with grain size variants due to different grain curvatures. It is observed from Figure 26 that at a grain size of 20nm different activation volumes were revealed for the grain size variants. From the different activation volumes revealed at a grain size of 20nm the activation volumes were lower for lengths measured along r_3, r_1

and r_2 whereas it was higher along r since the grain curvature of r was lower than the curvatures of r_3, r_1 and r_2. It was observed at a grain size of 40nm that the activation volume decreased when measured along r_3 and r_1 whereas it increased along r and r_2 due to higher grain curvatures of r_3 and r_1 and lower grain curvature of r and r_2. It was also observed at a grain size of 60nm to 80nm that the activation volume increased along r and decreased along r_1, r_2 and r_3. It is further observed at a grain size of 100nm that the activation volume decreased along r, r_1, r_2 and r_3. The results in Figure 26 revealed an increase and decrease of activation volume due to different grain curvatures on grain size variants. However, the smooth transition of activation volume for the grain size variants at different temperatures cannot be ignored as the obtained results revealed transition at different temperatures from negative activation volumes as temperature increased on the grain size variants.

4.19 Data from Mechanical testing (Tensile test) and Experimental cycles

Cycles	Elongation [nm]	yield Stress [MPa]
Initial Pass	7.856E-08	143
Passes	9.163E-08	220
Passes	4.502E-07	350
Passes	0.00013	150

Table 4: Yield stress from tensile test and Elongation from theoretical Simulation

It was observed that the yield stress increases with an increasing number of experimental cycles during experimentation as shown in table 4. The increase in yield stress during tensile testing revealed that nanomaterials have more enhanced properties when compared with conventional materials. During material deformation by ARB cycles, the material is subjected to straining. The straining in the material increases since several experimental cycles were performed. The increase in strain during experimentations impact the yield stress and elongation. The elongation were obtained by measuring the different directions of r_1, r_2, r_3 and r in the microstructures during deformation of the materials. It was also observed that continuous refinement did not lead to property enhancement as the material strength later decreased with an increasing number of passes as shown in table 4. The theoretical results agree with experimental results since there exists some correlation between both theoretical and experimental results as demonstrated in this dissertation.

CHAPTER FIVE

5.1 SUMMARISING CONCLUSSIONS AND RECOMMENDATION

The primary purpose of this study was to investigate on the acceptable procedure for modeling and design of nanomaterials' mechanical properties that are suitable under given set of conditions. In order to fulfill this purpose, relevant mathematical models were identified from literature survey. The identified models were the models of yield stress, young's modulus, strain rate sensitivities, elongation and size variants.

From the literature survey it was noted that, ARB and ECAP are severe plastic deformation techniques that are acknowledged to produce elongated grains during deformation of conventional materials to nanostructured materials. *It is very important to note that, most researchers have reported that, the grains deformed by ARB and ECAP are elongated*. It was also observed that the previous models relating grain size to properties considered only the equivalent radius measurement. Parameters such as semi minor axis length, semi major axis length and major axis length that determine true grain shape, elongation and size were not considered. It is from the above-mentioned observation that, models of grain elongation for 2-D grain, 3-D grain, SRS models of grain size variants and deformation activation volume for grain size variants were developed. The identified model of yield stress, young's modulus and strain rate sensitivities were modified/verified for 2-D grain and 3-D grain. Furthermore, the stochastic natures of the grain size variants were also taken into consideration since grain sizes in nanomaterials are random in nature.

From the developed models, different approaches of measuring nanomaterials' mechanical properties revealed different results. Since different approaches exists for measuring nanomaterials' mechanical properties that revealed different results, it is now understandable why there are several controversies when comparing different results of nanomaterials' mechanical properties. This is an indication that the published results might be correct although differences exist when comparing the different results. Some of the new findings on nanomaterials' mechanical properties might have been rejected although they exposed accurate results which may be of great value since different approaches might have been undertaken.

5.2 Conclusion

Based on the results of this study, a number of conclusions were drawn. From the results of 2-D grains it can be concluded that elongation was observed to have impact on properties during grain refinement. It was shown that the plots for yield stress as a function of different parameters showed more enhanced properties with the highest for elongation followed by the semi major axis length r_1 equivalent radius r and semi minor axis length r_2.

From the results of 3-D grains it was shown that properties varied in different ways with equivalent radii, semi

minor axis length, semi major axis length and major axis lengths. The present analysis revealed that the material had the most enhanced properties for lengths measured with higher grain curvature and lower for lengths with low grain curvature. It has also been revealed that in order to increase the material yield stress, the rate of straining of the material had to be reduced. It was also observed that, materials with elongated grains had more enhanced properties that rapidly dropped with continuous lengthening of the grains. The present analysis for 3-D grains shows more properties for nanomaterials which were not revealed from the models that dealt only with the equivalent radius.

From the SRS, it can be concluded that the effects of deformation temperature led to different SRS values due to different grain curvatures of the grain size variants. It was also observed that the SRS of the grain size variants decreased and increased with increasing temperature. The increase and decrease in SRS with temperature on the grain size variants suggests that the SRS for 6082T6 aluminium at the low and the high temperature ends are different. This indicates that different dynamic strain aging (DSA) mechanisms dominated the behaviour of the grain size variants at different temperature ranges since at extremely low temperature the SRS was small and at high temperature the SRS increased and resulted to material hardening. It can be concluded that increased in temperature impacted the SRS of nanostructured during grain refinement.

From the study of the effect of processing temperatures on activation volume for grain size variants, it can be concluded that the activation volume characterizes the stress sensitivity of dislocation velocity. This was also based on the thermally activated plastic deformation process of grain size variants, and the dislocation velocity also depended on the activation energy and the shear stress acting on the dislocation. These activities were characterized by different grain curvatures of grain size variants during grain refinement.

The deformation temperature led to different activation volumes on the grain size variants due to different grain curvatures. It was also observed that the activation volume of the grain size variants decreased and increased with increasing temperature. It can also be concluded that increased in SRS led to decrease in activation volume whereas increased in activation volume led to decrease in SRS due to different grain curvatures.

5.3 Recommendation and Direction of Further Studies

Though materials properties were enhanced during grain refinement, the different results of "*yield stress", "strain" and "strain rate"* as functions of the semi major axis length r_1, equivalent radius r, semi minor axis length r_2 and major axis length r_3 at the same grain size is an indication of controversy which require further study. It can be concluded that deformation of materials leads to different mechanical properties when considered as a function of the grain size variants. These findings provide valuable insights into the possibility of tailoring structure, and in particular grain size, to elicit desired properties in the material.

REFFERENCES

ANTON, S., BRANE, S. & MATEYZ, F. 2009. Determination of the strain-rate sensitivity and the activation energy of deformation in the superplastic aluminium alloy Al-Mg-Mn-Sc. *RMZ – Materials and Geoenvironment, Vol. 56, No. 4, pp. 389–399, 2009*

ARENAS, A., J., SILVA, V., Y., ALVA, M., J., & RIVERA, M. 2010. Advantages and limitations of OM, SEM, TEM, and AFM in the study of ancient decorated pottery. *Applied Physics A 2010 Vol.98 (3) pp 617-624*

ARMSTRONG, R.W. & RONALD, W. 2009. Strength and strain rate sensitivity of nanopolycrystals. *Invented for Mechanical Properties of Nanocrystalline Materials,* 19: 1-34.

BARR, D., L. & BROWN, W., L. 1995. A channel plate detector for backscatter diffraction. *Rev. Sci. Instrum. 66, 3480 (1995)*

BRAD, L., B., THOMAS, B., C. & MORRIS, F. D. 2007. The Strain-Rate Sensitivity of High-Strength High-Toughness Steels. *Sanddia Report Sand 2007-0036*

BHADESHIA, H. 2013. The first bulk nanostructured metal. *Science and Technology of Advanced Materials, 14: 1-7.*

CAI, W. & BELLON, P. 2013. Subsurface microstructure evolution and deformation mechanism of Ag-Cu eutectic alloy after dry sliding wear. *Wear 303 (2013)602–610*

CHARLES C.F. KWAN & WANG. 2010. Cyclic deformation behavior of ultra-fine grained copper processed by accumulative roll-bonding. *Procedia Engineering 2(2010)101-110*

CHE, B. T. & SCHWEGLER-BERRY, D. & CUMPSTON, A. & CUMPSTON, J. & FRIEND, S. & STONE, S. & KEANE, M. 2016. Performance of a scanning mobility particle sizer in measuring diverse types of airborne nanoparticles: Multi-walled carbon nanotubes, welding fumes, and titanium dioxide spray. *J Occup Eviron Hyg. 2016 (7):501-18*

CHIOU, S. T., TSAI, H. L. & LEE, W. S. 2009. Impact mechanical response and microstructuralevolution of Ti alloy under various temperatures. *J Mater Process Technol2009;209(5):2282–94.*

CUENOT, S., FRETIGNY, C., DEMOUSTIER, S. & NYSTEN, B. 2004. Surface tension effect on the mechanical properties measured by atomic microscopy. *The American Physical Society, 69(16):1-5, 20.*

ESTRIN, Y. & VINOGRADOV, A. 2013. Extreme grain refinement by severe plastic deformation. A *Wealth of Challenging Science: Act materials, 61: 782-817.*

GREGER, M., KOCICH, R. & CIZEK, L. 2006. Grain refining of Cu and Ni-Ti shape memory alloys by ECAP process. *Journal of Achievements in Materials and Manufacturing Engineering volume 20 issues 1-2 January-February 2007.*

GUNDEROV, D. V. & MAKSUTOVA, G. & CHURAKOVA, A. & LUKYANOV, A. & KREITCBERG, A. & RAAB, G. I. & SABIROV,A.I. & PROKOSHKIN, S. 20015. Strain rate sensitivity and activation volume of coarse-grained and ultrafine-grained TiNi alloys. *ScriptaMateriallia 102 (2015) 99-102*

GUNTER, H., RONTGENOPTIK & RONTGENOTIK. 1965. X-ray microscopy. *Fortschritte der Physik, Vol.4. pp (1-32)*

GUISBIERS, G. 2010. Size dependent materials properties towards a universal equation. *Nanoscale Research Letters, Vol. 5, No.7, pp. 1132-1136*

GUOFENG, WANG. & XIAODONG. 2008. Predicting the young's modulus of nanowire from first principle calculations on their surface and bulk materials.*J. Appl. Phys. 104, 113517(2008)1-33*

HALL, E. O. 1951. The deformation and ageing of mild steel. III discussion of results. *Proceedings of the Physical Society, Section B, 64(9): 747-753.*

HASLAM, A. J. & MOLDOVAN, D. & PHILLPOT, S. R. & WOLF, D. & GLEITER, H. 2002. Combined atomistic and mesoscale simulation of grain growth in nanocrystalline thin films. *Computational Material Science 23 (2002) 15-32.*

HERMANN, M.., BIRGIT, W., OLIVER, F., HAN, H., THOMAS, K. & LIU, W. 2007. Particle counting efficiencies of new TSI condensation particle counters. *Journal of Aerosol Science 38(6):674-682*

HIDALGO, P. M. & CEPEDA, J. C. M. & RUANO, O. A. & CARRENO, R. O. A. 2012. Effect of warm accumulative roll bonding on the evolution of microstructure, texture and creep properties in the 7075 aluminium alloy. *Mater SciEng A 556 (2012) 287-294 DOI 10.1016/j.msea.2012.06.089*

HILLERT, M. 1965. On the theory of normal and abnormal grain growth. *Acta Metal. 13, pp.227, (1965)*

HOFMANN, *H*. 2011. Course 4(pdf)-LTP/EPFL.Advanced Nanomaterials; H. Hofmann, version 2011.1.1. MECHANICAL PROPERTIES.1.1. [Online]. Available at: *<htp:ltp.epfl.ch/files/...advancednanomaterials/.../MechanicalProperties.pdf>. Accessed: 12/03/2013.*

HUANG, X. & TSUJI, N. & HANSEN, N. & MINAMINO, Y. 2003. Microstructural evolution during accumulative roll-bonding of commercial purity aluminum. *Mater. Sci. Eng. A* 2003, *340*, 265–271.

JONATHAN, P. R., KINGSLEY, J. & JASON, S. 2013. The CPMA electrometer system-a suspended particle mass concentration standard. *Aerosol Research Letter Vol. 47(8)2013.*

KREITCBERG, A., PROKOSHKIN, S., BRAILOVSKI, V., GUNDEROV, D. & KHOMUTOV, M. 2014. Influence of the strain rate and deformation temperature of the deformability of Ti – Ni SMAs: A preliminary study. *Material Science and Engineering 63(2014)012109*

KUMAR, R., SHARMA, G. & KUMAR, M. 2013. Effect of size and shape on the vibrational and thermodynamics properties of nanomaterials. *Journal of thermodynamics Vol. pp 5*

KIM, Y. S., LEE, T. O., & SHIN, D. H. 2004. Microstructural Evolution and Mechanical Properties of Ultrafine Grained Commercially Pure 1100 Aluminum Alloy Processed by Accumulative Roll-Bonding (ARB). *Mater. Sci. Forum* 2004, *449–452*, 625–628.

KWAN, C., WANG, Z., & KANG, S. B. 2008. Mechanical behavior and microstructural evolution upon annealing of the accumulative roll-bonding (ARB) processed Al alloy 1100. *Mater. Sci. Eng. A* 2008, *480*, 148–159.

LASZLO, S. TOTH & CHENGFAN GU.Ultrafine grain metals by severe plastic deformation. *Material Characterization 92(2014) 1-14*

LEE, W. S. & LIN, C. F. &CHEN, T. H. & HWANG, H. H. 2008. Effects of strain rate and temperature onmechanical behavior of Ti–15Mo–5Zr–3Al alloy. *J MechBehav Biomed Mater 2008;1(4):336–44.*

LEWANDOWSKA, M., PAKIELA, Z., GARBACZ, H., WIENCEK, D. A., ZIELINSKI, W. & KURZYDLOWSKI, J. K. 2006. Structure and properties of nanomaterials by severe plastic deformation.*In the Proceeding ofNukleonika*, 51(1): 19-25.

LEWANDOWSKA, M. 2006. MalgorzataLewandowska: Fabrication methods of nanomaterials. *Structure and Properties of Nanomaterials, 1-54.*06[CD-ROM].

LIMIN WANG &ZHENBO WANG & SHENG GUO & KE LU. 2012 Annealing-induced grain refinement in a nanostructuredferritic steel. *J. Mater. Sci. Technol., 2012, 28(1), 41-45*

LINLI ZHU & HAIHUI RUAN & XIAOYAN LI & MING DAO & HUAJIAN GAO & JAIN LU. 2011. Modeling grain size dependent optimal twin spacing for achieving ultimate high strength and related high ductility in nanotwinned metals. *Act Materialia 59 (2011) 5544-5557*

LI, B. L. & TSUJI, N. & KAMIKAWA, N. 2006. Microstructure homogeneity in various metallic materials heavily deformed by accumulative roll-bonding. *Mater. Sci. Eng. A* 2006, *423*, 331–342.

MASAYOSHI, N. 2002. The science of color. *Baifukan (2002) p. 108*

MAY, J., HOPPEL, H. W. & GOKEN, M. 2005. Strain rate sensitivity of ultrafine-grained aluminium processed by severe plastic deformation. *ScriptaMaterialia 53(2005)189-194*

MEIER, M. 2004. The hall petch relationship. Lecture notes: *Department of Chemical Engineering and Materials Science University of California, Davis, 1-17.*

MEYER, M., MISHRA, A. & BENSON, D. J. 2006. Mechanical properties of nanocrystalline materials. *Progress in Nanomaterials Science*, 51:427-556, 1.

MORRIS, D. G. 2010. The origins of strengthening in nanostructured metals and alloys. *Revista de Metalurgia,*46(2): 173-186.

PETCH, N. J., 1953. The cleavage strength of polycrystasl, J. *Iron and Steel Institute, 174: 25-28.*

PICU, R. C. & VINCZE, G. & OZTURKA, F. & GRACIO, J. J. & BARLAT, F. & MANIATTY, A. M. 2004. Strain rate sensitivity of the commercial aluminum alloy AA5182-O. *Materials Science and Engineering A 390 (2005) 334–343*

RAHMAN, K. M. & VORONTSOV, V. A. & DYE, D. 2015. The effect of grain size on the twin initiation stress in a TWIP steel. *ActaMaterialia 89(2015) 247-257*

ROSOCHOWSKI, A. & OLEJNIK, L. & RICHERT, J. & ROSOCHOWSKA, J. & RICHERT, M. 2012. Equal channel angular pressing with converging billets-experiment. *Materials Science & Engineering A 560(2013)358-364*

SABIROV, I. & BARNETT, M. R. & ESTRIN, Y. & HODGSON, P. D. 2009. The effect of strain rate on the deformation mechanisms and the strain rate sensitivity of ultra-fine-grained Al alloy. *ScriptaMaterialia 61(2009) 181-184*

SARAVANAN, M. & PILLAI, R, M. & PAI, B, C. & BRAHMAKUMAR, M. & RAVI, K, R. 2006. Equal channel angular pressing of pure aluminium-an analysis. *Mater. Sci, Vol. 29, No. 7, pp. 679-684.*

SAITO, Y., TSUJI, N., UTSUNOMIYA, H., SAKAI, T. & HONG, R. G. 1998. Ultra-fine grained bulk aluminium produced accumulative roll-bonding (ARB) process. Department of Material Science and Engineering Osaka University Japan. *ScriptaMaterialia, 39:1221-1227*

SEGAL, V. M. 2005.Deformation mode and plastic flow in ultra-fine grained metals.*Materials Science and Engineering A 406(2005)205-216*

STEVEN INSTITUTE. 2008. 2028 Vision for mechanical engineering.*A Report of the Global Summit on the Future of Mechanical Engineering, 1-23.*

TAMIMI, S.**,** KETABCHI, M. & PARVIN, N., 2008. Microstructural evolution and mechanical properties of accumulative roll bonded interstitial free steel. Department of Mining and Metallurgical Engineering, Amirkabir University of Technology, Tehran, Iran. *Materials and Design 30(2009)2556-2562.*

TEGEN, T. B, WEJRZANOWSKI, IWANKIEWICZ, R. & KURZYDLOWSKI, J. K. 2008.The effects of grain size distribution on nanmaterials mechanical properties, *Solid State Phenomena, 140: 185-190.*

TENGEN, T. B. 2008. *Analysis of Characteristic of Random Microstructures of Nanomaterials*. PhD. Thesis. Witwatersrand Johannesburg.

TENGEN, T. B., WEJRZANOWSKI, T., IWANKIEWICZ, R. & KURZYDLOWSKI, K. J. 2010. Stochastic modelling in design of mechanical properties of nanometals. *Materials Science and Engineering A, 257: 3764-3768.*

TENGEN, T. B. 2011. Designing nanomaterials with desired mechanical properties.*Nanoscale Research,*6(1): 585.

TENGEN, T. B. 2010. Designing nanomaterials' mechanical properties from the observable nanostructure features. *NSTI – Nanotech, 2:661-664*.

TENGEN, T. B. 2012. Stochastic effect of strain-rate sensitivity on nanomaterials' mechanical properties. Programme of Eight South African Conference on Applied Mechanics 2012 (SACAM 2012) 3-5 September 2012. Organised and hosted by Mechanical Engineering Science of the University of Johannesburg South Africa. pp 198 – 202.

TENGEN, T. B. & IWANKIEWICZ, R. 2009.Modelling of the grain size probability distribution in polycrystalline. *Composite Structures 91(2009) 461-466*

TSUJI, N., SAITO, Y., HEE LEE, S. &MINAMINO, Y. 2003. ARB (Accumulative roll bonding) and other new techniques to produce bulk ultrafine grained and materials.*Advanced Engineering Materials 5 No 5*

VAN SWYGENHOVEN, H. & SPACZER, M. & CARO, M. 1999. Microscopicdescription of plasticity in computer generated metallic nanophasesamples: a comparison between Cu and Ni.*Acta Mater.47,3117(1999).*

VASCO, F. & ANDREA, H, & WIM, J. 2010. Critical evaluation of nanoparticle tracking analysis (NTA) by nanosight for the measurement of nanoparticles and protein aggregates. *Pharm Res. 2010 (27(5):796-810)*

WANG, Z. J. & SHAN, Q. J. & SUN, L. J. & MA, E. 2012. Sample size effects on the large strain bursts in submicron aluminum pillars. *Applied Physics Letters 100, 071906*

WANG, Y. B. & HO, J. C. & LIAO, X. Z. & LI, H. Q. & RINGER, S. P. & ZHU, Y. T. 2009.Mechanism of grain growth during severe plastic deformation of a nanocrystalline Ni–Fe alloy. *APPLIED PHYSICS LETTERS **94**, 011908 _2009_*

WILLIAM A. NASH. (4thed.). 1998. *Strength of materials.* New York: McGraw-Hill.

WHANG, H.S. (ed.). 2011. *Nanostructured Metals and Alloys*. UK: Woodhead Publishing.

XIONG, S., Qi, W., CHENG, Y., HUANG, B., WANG, W. & LI, Y. 2011. Universal relation for size dependent thermodynamic properties of metallic nanoparticles. *Physical Chemistry Chemical Physics, Vol. 13, No. 22, pp. 10652-10660*

ZHANG, W. & ZHANG, D. 2010. Production of Mg-Al-Zn magnesium alloy sheets with ultrafine-grain microstructure by accumulative roll-bonding. *Transaction of Nonferrous Metals Society of China, 21(2011)991-997*

ZHANG, M. LI, C. ZHANG, W & ZHANG, D. 2012. Processing of AZ31 magnesium alloy by accumulative roll-bonding at gradient temperature. *Acta Metall. Sin(Engl. Lett.) vol.25 no1 pp65-75 February 201*

ZHANG, Z. & LII, X. X. & JIANG, Q. 1999. Finite size effect on melting enthalpy and melting entropy of nanocrystals. *Physical B Vol. 270, No. 3-4, pp. 249-254*

ZHAO, M. & JIANG, Q. 2006. Reverse hall-petch relationship of metals in nanometer size. *Emerging Technologies-Nanoelectronics, IEEE Conference on Vol. pp 472-474, (10-13 Jan. 2006)*

ZHOU, C. & BEYERLEIN, I. J. & LESAR, R. 2011. Plastic deformation mechanisms of fcc single crystals at small scales. ActaMateraillia 59 (20), 7673-7682

ZHU. T, & LI. J, & SAMANTA. A, & LEACHE. A, & GALL, K. 2008. Temperature and strain rate dependence of surface dislocation nucleation. Physical Review Letters 100 (2),025502

APPENDIX

r=r0+integral(b*r,time,0,1000)
r_2=r0*(1-Ratio_2)+Ratio_2*r
r0=100
c=1.1
b=-0.0035
r_3=Ratio_1*r_1+(1-ratio_1)*r0
r_1=r0+integral(M*(PC-1)*r_12/r_1^3-A*r_1*v_1,time,0,1000)

r_12=r120+integral(2*M*(PC*r_12/r_1^3-1)+D^2*r-(2*A+A^2)*r_1^2*v_1,time,0,1000)
r120=100
"ar_1=1/2*r_1"
D=1/10000
A=0.4
Ratio_1=0.81
Ratio_2=01.071

Y=S00+A_2*(r^(-1/2))-B_2*(r^(-1))-C_2*(r^(-3/2))
strainr=integral(r0,time,0,1000)+integral(r,time,0,1000)+integral(b*r,time,0,1000)
strainr3=integral(Ratio_1*M*(PC-1)*r_1^3/r_1^8+r*(D),time,0,1000)+integral(r0,time,0,1000)
strainr1=integral(M*(PC-1)*r_1^3/r_1^8+r*(D)+A*r_1*v_1,time,0,1000)
strainr2=integral(r0*(1-Ratio_2)+Ratio_2*r,time,0,1000)
strainrater1=strainr1/(time+0.000001)
strainrater2=strainr2/(time+0.000001)
strainrater3=strainr3/(time+0.000001)
strainrater=strainr/(time+0.000001)
ELONGATION=(P*r_1)/(3/4*180*r^3)*(E)

E=(P)/(r-r_0)*(r^3)^(2/3)/(192*I) "young's modulus"
I=(22/7*r_1^4)/64
P=1
r-r_0=d

A_2=K_d
B_2=2*K_t*h_0*H_m/(K*T_r)
C_2=2*K_d*h_0*H_m/(K*T_r)
S00=16.7
K_d=1301.77
K_t=1.93
T_r=300
v_1=T_1*r_1^2

T_1=0.000008

PC=1.95

M=M_0*(1+CD*r_12/r_1^3)

M_0=M_01*exp(-T_m_inf/T)

M_01=1E-3

T_m_inf=933.47

T=700

CD=(4*H_m*h_0)/(K*T)

H_m=10710

h_0= 0.25

K=8.314472

$Integral time,
r,r_2,r_3,r_1,Y,strainr,strainr1,strainr2,ELONGATION,strainrater1,strainrater2,strainrater3,strainrater